ORTHOGONAL PATTERNING OF BLOCK COPOLYMER

A Thesis

Presented to the Faculty of the Graduate School

of Cornell University

In Partial Fulfillment of the Requirements for the Degree of

Master of Science

by

Yefei Zhang

August 2012

ABSTRACT

Block copolymer self-assembly presents a method for pattern and template application on the 10 to 50 nm length scale. However, the research in this area has been limited to the use of only one block copolymer per layer due to the damage and intermixing when spin coating of a second polymer layer. Here we propose a new method that neatly solves the intermixing problem by using a fluorinate photoresist and solvent system. The microdomain orientation within the block copolymer film can be controlled by solvent vapor annealing. And we also observed an improvement of the long-rang order of the microdomains by depositing the block copolymer into lithographical patterned trenches. This orthogonal patterning method allows for the deposition of multiple block copolymers, with ordered microdomains, adjacent to each other on the same layer. The self-assembled patterns can be transferred to the substrate and propose a potential route for the next-generation lithography.

BIOGRAPHICAL SKETCH

Yefei Zhang was born to Zhi Zhang and Hua Song on June 20th, 1987. From his early age, his parents, two chemical engineers at the biggest automobile manufacturing factory in China, cultivated in him an interest in engineering. After completing his high school study, he passed the national entrance exam and chose to study Materials Science and Engineering at Jilin University. In his junior year, he entered Prof. Jingyuan Wang's lab at Department of Chemistry to conduct some basic experiments in polymer science and this experience made him dedicated to polymer materials.

After earning his bachelor degree in 2010, wanted to escape from Changchun, the city where he lived for more twenty years, and to acquire a higher-level education, he tried to apply for graduate schools in the U.S. He was fortunate to be accepted into the Materials Science and Engineering Department at Cornell University, where he pursued his M.S. degree under Prof. Christopher Ober's supervision. The two years of study and research at Cornell changed his view of science and engineering, and trained him in scientific research. He completed his M.S. degree in July 2012, and this was just a start of his scientific life. He will continue his PhD study in Prof. Stuart Rowan's group at Macromolecular Science and Engineering department, Case Western Reserve University, starting in the fall of 2012.

ACKNOWLEDGMENTS

First and foremost, I would like to thank my parents, Zhi Zhang and Hua Song. Without their continuously encouragement and support, I cannot finish my master degree at a world famous university and to be where I am today. Second, I would like to thank Prof. Christopher Ober, who was kindly enough to accept me into his research group. His scientific insight, supervision and encouragement during my master study left a deep impression on me and trained me to be a scientific researcher. I would also like to take this chance to thank Prof. Michael Thompson for serving on my thesis committee, and for his helpful suggestion towards the completion of my degree.

The Ober group felt like home and I have got tremendous help from the other group members during the past two years. I would like to thank Carol Newby for all her helps with my experiments. I would also like to thank all my other friends in the Ober group: Prof. Claudio dos Santos, Dr. Evan Schwartz, Dr. Joan Bosworth, Dr. Drew Forman, Dr. Harihara Subramanian, Dr. Youyong Xu, Dr. Nam Ho You, Dr. Hee-soo Yoo, Dr. Heloise Therien-Aubin, Dr. Yosuke Hoshi, Dr. Christian Ohm, Dr. Yeon Sook Chung, Dr. Kui Xu, Dr. Yisheng Xu, Michelle Chavis, Jing Jiang, Zhaoli Zhou, Lin Chen, Christine Ouyang, Liz Welch, Alwin Wan, Marie Krysak, Brandon Wenning, David Calabrese, Katherine Camera, Byungki Jung, Rina Maeda and Xiangyu Li and all the other present and former group members for their support and friendship.

I would also like to acknowledge all those non-Ober group friends: Yibei Gu, Yan Kang, Lin Xu, Dr. Gengeng Qi, Dr. Zihui Li, Xiaonan Duan, Ian Fuller and Rebecca Schur for advices and being friends.

TABLE OF CONTENTS

LIST OF FIGURES

CHAPTER 1

CONTROL OF ORIENTATION AND LONGE-RANGE ORDER WITHIN SELF-ASSEMBLED BLOCK COPOLYMER FILMS

1.1 Introduction

Block copolymers have received increasing interest due to their distinct ability to self-assemble and form features at nanometer length scales[1-15]. The architecture of a block copolymer, which consists of two or more homopolymer segments that are immiscible with each other, enables phase separation into periodic domains. Typical dimensions of the microdomains range from 5 to 50 nm, which is difficult to achieve using other materials and methods. These self-assembled structures can be further transformed to create templates that can be used in many research areas. For example, the continuous demand of smaller feature size in today's semiconductor industry has been limited by expensive equipment and materials[16]. It is extraordinarily difficult for conventional UV lithography to achieve pattern sizes smaller than 20 nm, while the microstructures formed spontaneously by block copolymers stand out as a promising tool for advanced lithography without the need to continuously invest money in expensive tools.

Self-assembly is facilitated by imparting mobility to polymer chains so they may move and reorient to form periodic domains whether in the melt, solid state or solution. This can be achieved by many methods, such as thermal annealing, solvent vapor annealing, or application of electric field and shear force. Thermal annealing is the most generally used technique involving heating the block copolymer above its glass transition temperature to induce long range order. Solvent vapor annealing is another effective method for block copolymer systems that are not capable with thermal annealing. The solvent vapor acts as plasticizer by swelling the polymer

domains and thus lowering the glass transition temperature of the system, enabling a phase separation to occur.

However, many applications of block copolymer self-assembly have been restricted by lack of spatial control over the periodic microdomains formed by a block copolymer. It critical in block copolymer self-assembly applications to understand how to pattern microdomains, to achieve registration and to determine the degree of order achieved. In this chapter, we briefly overview some commonly used techniques to control and pattern the block copolymer microdomains in order to fulfill different requirements regarding their application in different areas.

1.2 Block copolymer phase behavior

Block copolymers are a specific class of copolymer that consist of two or more distinct polymer segments covalently bound to each other to form a single chain[17]. The simplest form is the linear AB diblock copolymer in which two homopolymer chains are bonded covalently in the center. The diblock copolymer system has been studied extensively for its ability to phase separate and form microstructures both experimentally and theoretically[18-21].

The two segments of diblock copolymer tend to demix while the covalent bonds in the middle of the chain prevent macroscopic phase separation. The repulsive interaction is characterized by the value of χN, where χ is the Flory-Huggins interaction parameter and N is the degree of polymerization[22]. When χN exceeds a critical value, a microphase separation can be observed until equilibrium is established. For strongly segregated polymers, the equilibrium morphology is

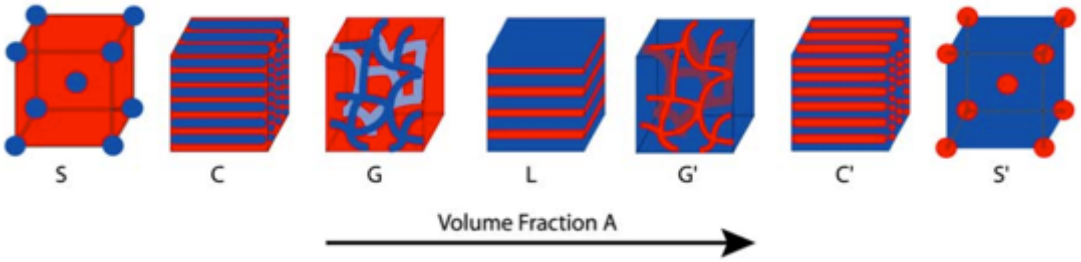

Figure 1.1 Equilibrium morphologies by phase separating of diblok copolymer. With increasing volume fraction f of phase A (blue), the morphology can be sphere, cylinder, gyroid and lamellae (Adapted from ref. 11. Copyright 1999 American Institude of Physics).

determined by the volume fraction *f* of one block[20]. Figure 1.1 shows schematic morphologies of a typical diblock copolymer system predicted by self-consistent mean-field theory. This theory is based on the balance between the repulsive polymer-polymer interactions versus the elastic restoring force energy for a particular microphase structure[23]. The results of these calculations can be converted and plotted as a phase diagram, as shown in Figure 1.2.

The size of the periodic microdomain scales with the molecular weight of the block copolymer. The period spacing L_0 is found to follow the power law $L_0 \sim N^{\alpha}$, where α is equal to 2/3 for the strong segregation limit (SSL), 1/2 for the weak segregation limit (WSL) and varies between 0.8 to 0.83 in the intermediate segregation regime (ISR)[23-26]. A typical scale of the morphology ranges from 20 to 50 nm[27]. It is difficult for high molecular weights polymer to phase separate due to entanglement and limit chain mobility. The smallest feature size is limited by a small value of χN (N is small for low molecular weight polymer), which means a lack of sufficient driving force for phase separation to take place.

1.3 Control of microdomain orientation and long-range order

There have been numerous reports utilizing a self-assembled block copolymer nanostructure as nanoreactors, nanoporous matrices, as well as templates for subsequent high-resolution lithography. For many technical applications, long-rang order of domain orientation is necessary. However, the microdomains in the bulk state normally have grain size of about a micron and have

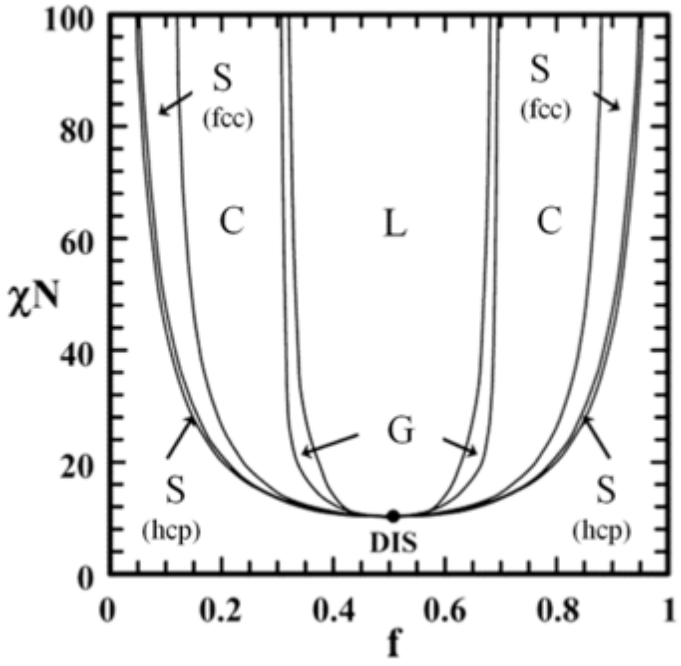

Figure 1.2 An illustration of a hypothetical phase diagram for block copolymers, with the volume fraction plotted as a function of the Flory-Huggins interaction parameter χN, with symbols corresponding to the morphologies shown in Figure 1.1. (Adapted from ref. 23. Copyright 2006 American Chemical Society.)

random orientations, which is not useful. Therefore, various strategies have been used for achieving large area orientation of block copolymer microdomains.

1.3.1 Control of film thickness and surface properties

When block copolymers form thin films on a substrate, the morphology is affected by the film thickness as well as the substrate/polymer and air/polymer interactions[28-35]. It has been found that a symmetric PS-*b*-PMMA diblock copolymer will form lamellar microdomains that orient parallel to the surface when deposited on a native oxide surface of a silicon wafer. The PMMA wets the silicon substrate since the polar block of PMMA prefers to make contact with the hydrophilic oxide surface, while the PS lamellae assemble at the air interface due to a lower surface energy of the non-polar PS block[28].

Despite the preferential wetting of the surface, the film thickness has also been found to influence the morphology formed by the PS-*b*-PMMA diblock copolymer system[36, 37]. When the film thickness is commensurate with the periodic spacing L_0 of the block copolymer (thickness=(n+1/2) L_0), the lamellar morphology will form parallel to the substrate surface as described above[28]. However, if the film thickness doesn't follow this relationship, a unique island and hole structure is formed to minimize the total energy by quantizing the local film thickness. However, Morkved and Jaeger observed a change in the orientations of the lamellar morphology when the films thickness is about equal to the block copolymer periodic spacing (thinkenss~L_0)[38, 39]. As we can see from Figure 1.3 a, the lamellar

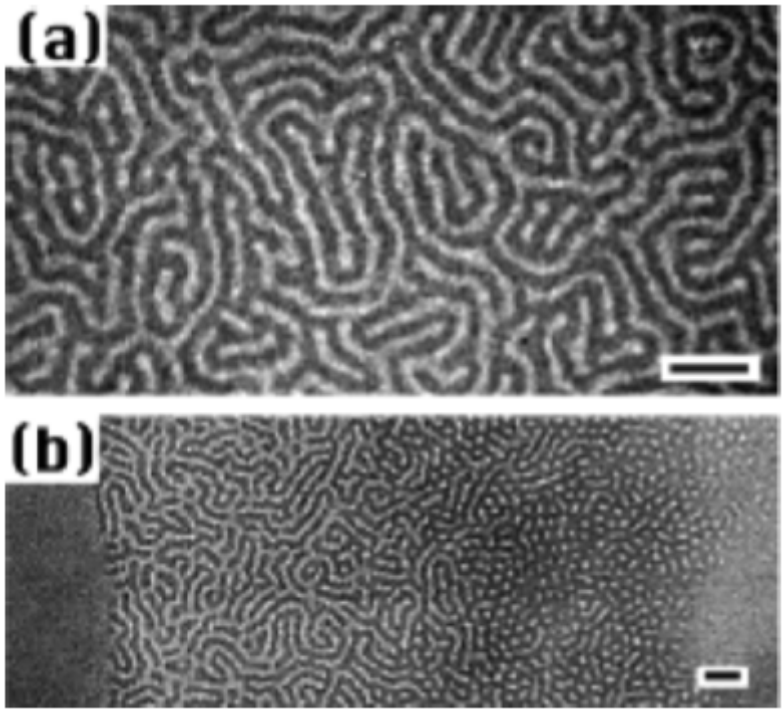

Figure 1.3 TEM images of symmetric PS-PMMA. Light domains correspond to PMMA and dark domains to PS. (a) Uniform thickness $t=L_0$. (b) Coexisting morphologies in a film with thickness gradient range from 3/2 L_0 (left) to 1/2 L_0 (right). (Adapted from ref 38. Copyright 1997 EDP Sciences.)

morphologies arise from the substrate and form perpendicular orientations within a film as thick as L_0 after annealing at 155 °C. While for a film containing a thickness gradient from 1/2 to 3/2 L_0, they observed coexistence morphologies of perpendicular lamella and disordered PMMA domains.

1.3.2 Application of external fields

External fields have been widely used to align the block copolymer microdomains with their ability to tune the microstructure and control long-range order in the bulk state.

1.3.2.1 Thermal annealing and temperature gradient

For applications in lithography, the block copolymer is generally spin-coated on top of a silicon substrate. However, the rapid evaporation of the solvent during the spin coating step leaves a non-equilibrium microstructure with random order. Thus, a subsequent treatment of the block copolymer is important to remove the defects and tune the microstructure. Thermal annealing is the most commonly used technique carried out simply by heating the polymer film above the glass transition temperature of both blocks in order to provide the polymer chains enough mobility to move and reorient[40-45]. The temperature must be lower than the decomposition temperature of the block copolymer to avoid degrading of the blocks. Kramer and coworkers have found a best condition to thermal anneal PS-*b*-P4VP block copolymer by heating the film above the order-disorder transformation temperature[46]. At this condition, the polymer blocks mix with each other, remove

defects and forms larger grains. A very sharp interface between the blocks is formed upon phase separation by cooling the film below the order-disorder transformation temperature.

Even though thermal annealing can improve the morphology, it does nothing to help align the block copolymer microdomain to gain long-range order. Hashimoto and coworkers have shown that a sharp and slowly moving temperature gradient could be used to align PS-*b*-PI block copolymer[47-50]. This process is very similar to the "zone-refinement" method and a single-crystal-like lamellar grain was grown with the lamellae normal parallel to the temperature gradient. Jones and coworkers have also shown the utilization of a sharp temperature gradient (17 °C/mm) to anneal a cylinder forming PS-*b*-PMMA block copolymer[51, 52]. However, the annealing temperature is between the glass transition temperature and the order-disorder transformation temperature, the so called "cold zone annealing (CZA)". Figure 1.4 shows the AFM image after this CZA process at different moving velocity. For the sample moving at 1 μm/s (Figure 1.4 d), they observed an almost defect-free single-grain-like block copolymer microdomain with long-range order along the temperature gradient at a scale of 2 μm.

1.3.2.2 Solvent vapor annealing

For some block copolymers, it is not possible to use thermal annealing techniques since the decomposition temperature of the block is much lower than the glass transition temperature. Solvent annealing is an alternative way to gain

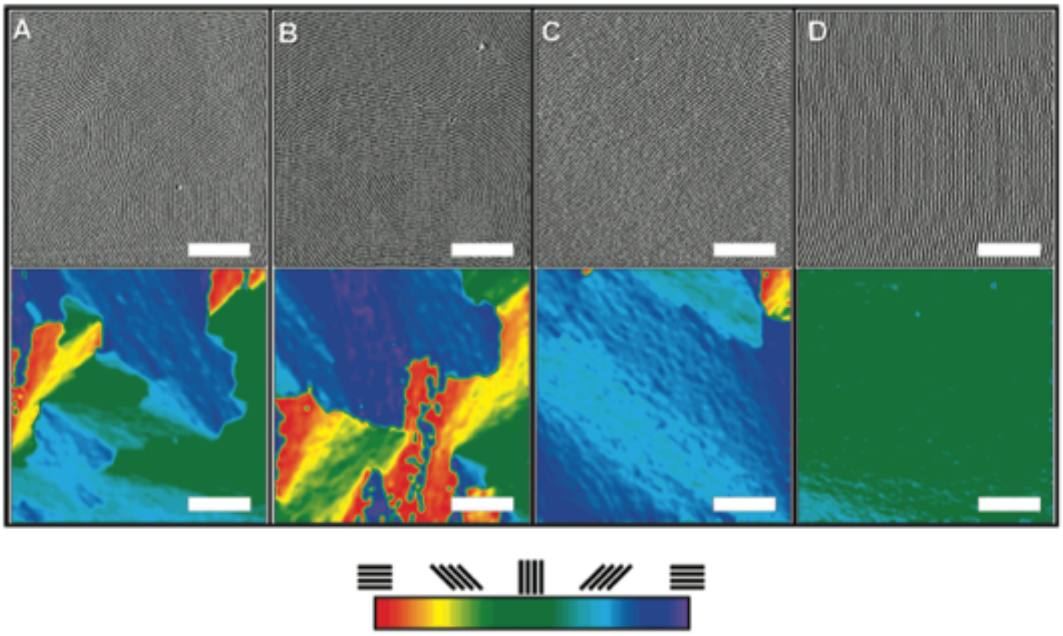

Figure 1.4 AFM phase images and cylinder orientation maps (below) of PS-*b*-PMMA films annealed with push velocity of a) 100 μm/s, b) 40 μm/s, c) 5 μm/s and d) 1 μm/s. Defect density decreases dramatically with decreasing velocity. Scale bars in all images are 500 nm. (Adapted from ref 51. Copyright 2007 American Chemical Society.)

polymer mobility without using heat. When the solvent vapor swells the polymer film, it acts as a plasticizer, which decreases the polymer's glass transition temperature. The polymer chains can gain mobility and are able to undergo an order-order transformation even below room temperature[53, 54]. An example is the low defect density perpendicular cylinder morphology achieved by exposing PS-*b*-PEO block copolymer to benzene and water vapor for two days[55].

Another great advantage of solvent vapor annealing over the thermal annealing is the ability to control the block copolymer domain morphology through a choice of solvents. For example, PαMS-*b*-PHOST block copolymer with a volume fraction 29 % of the PαMS block annealed in THF vapors formed a parallel oriented cylindrical morphology, while a spherical morphology is observed when the film is annealed in acetone vapor[56-58]. The reason for this is that THF is a good solvent for both blocks, while acetone is not a good solvent for PαMS blocks, though we have found it to be a good solvent for the PHOST homopolymer. Consequently, acetone will preferentially swell the PHOST block in the swollen state and induce the order-order transition from cylindrical to spherical morphology. The resulting morphology may be kinetically trapped in the dry state.

1.3.2.3 Application of electric field and shear force

Russell and coworkers have demonstrated that a vertically oriented cylindrical PMMA domain orientation by applying a DC electric field (30-40 V/μm) perpendicular to the film surface while heating the polymer film above its glass transition temperature[59]. They also proposed that the driving force for alignment is

the orientation-dependent polarizability of the original anisotropic microdomains.

Shear alignment is advantageous over other techniques since the process is simple and easily applicable to large areas. The response and dependence of spherical, cylindrical and lamellar microdomains to orientation under shear conditions have been extensively studied and established[60-63]. Angelescu and coworkers used shear flow to align polystyrene-*b*-poly(ethylene-*alt*-propylene) (PS-*b*-PEO) to form cylindrical and spherical PEP microdomains[64, 65]. PDMS was used to impose shear stress on the films with shear being applied at a temperature between the glass transition temperature and the order-disorder transformation temperature. The film contained single layers of PEP cylinders that can be aligned parallel to the shear direction with long-range order (Figure 1.5 a and b)[64]. But due to a lack of mechanical anisotropy in a hexagonal lattice, a single layer of spherical domain cannot be aligned by shear force. Two or more layers of spheres were required[65-67]. Shear alignment is good for applications that do not require perfect long-range orders.

1.3.3 Topographic patterning; Graphoepitaxy

The topographic guiding patterns, created by the conventional photolithography, can be utilized to help align the microdomain of the block copolymer to gain lateral order within the film.

Sibener and coworkers have reported a simple approach for spatial alignment of cylindrical microdomains using topographic patterns created by electron beam lithography and reactive ion etching (RIE)[68-70]. When an

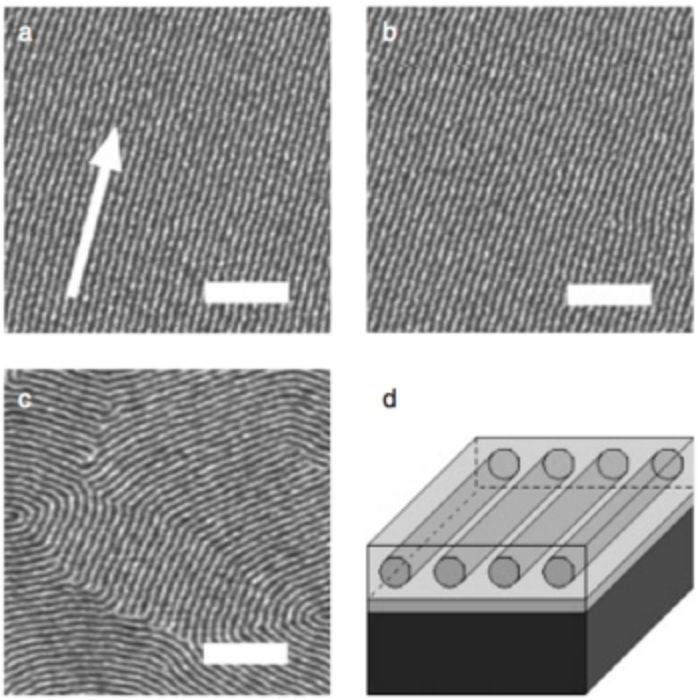

Figure 1.5 a) AFM image of polymer films by shear aligning. The arrow indicates the shear direction. b) Another image acquired 8 mm away from a). c) Polymer films annealed without shearing yields fingerprint-like patterns. d) Schematic of monolayer cylindrical microdomain. (Adapted from ref 64. Copyright 2004 Wiely-VCH.)

asymmetric PS-*b*-PEP block copolymer film is deposited on an unpatterned substrate, the polymer forms random fingerprint like cylindrical morphology with no long-range order. While aligning the block copolymer inside the topographic patterns, aligned cylinders parallel to the sidewall of the patterns forms. Aligned cylinders are observed on both troughs and crests of the patterns. Park and coworkers demonstrated control of perpendicular oriented lamellar microdomains by creating topographic patterns with tailored wetting properties[71]. When the bottom surface is neutral to both PS and PMMA blocks while the sidewalls are selectively wetted by one of the blocks, an orientation of lamellar domains parallel to the sidewall and perpendicular to the bottom surface is achieved (Figure 1.6 a). When both the sidewalls and the bottom are neutral for both blocks, the lamellar domains orient perpendicular to both the substrate and sidewalls (Figure 1.6 c). The perpendicularly oriented lamellar microdomains can be used to create line/space patterns for lithography applications. The dimension of the topographical features has also been shown to influence the microstructures of the block copolymer film[72-74].

1.3.4 Chemical epitaxy

Heterogeneous chemical surface patterns can also act as guides for the formation of well-ordered block copolymer microdomains. It must be taken into account that matching the length scale of the surface heterogeneity with periodicity is important to achieve low defect density morphologies[75]. The Nealey group has focused on using chemical patterns to direct the self-assembly of PS-*b*-PMMA block

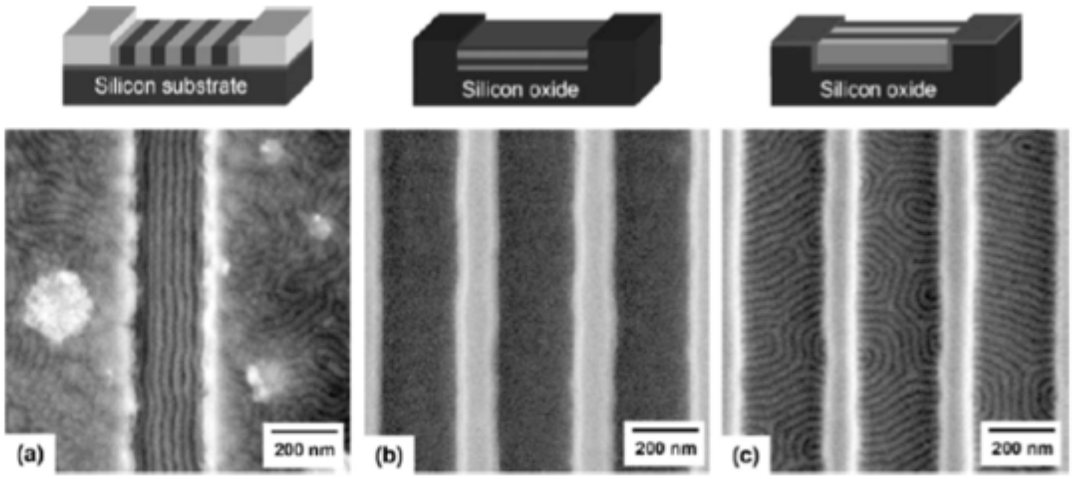

Figure 1.6 Lamellar structures of symmetric PS-*b*-PMMA on topographically patterned substrate. a) The sidewalls are preferentially wetted by the PS block, while the bottom surface is made neutral to both blocks. b) Lamellar microdomain orients parallel to the bottom surface. c) The sidewalls are treated with neutral brush and the lamellar morphology of b) transforms to perpendicular to both sidewall and bottom. (Adapted from ref 71. Copyright 2007 Wiley-VCH.)

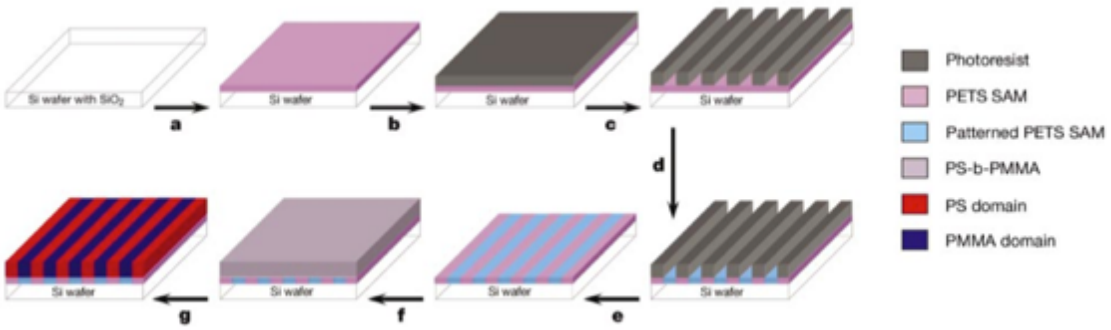

Figure 1.7 Schematic flow of the direct self-assembly using chemical guiding patterns. (Adapted from ref 79. Copyright 2003 Nature Publishing Group.)

copolymers[76-78]. The general patterning process is described in Figure 1.7[79]. They patterned the photoresist layer using extreme ultraviolet interferometric lithography (EUV-IL) and transferred the patterns to the underlying self-assembled monolayer (SAM). The resulting substrate has chemically patterned stripes of polar and nonpolar regions that could be used as sites to attract the PMMA and PS domains, respectively. Defect-free alignment of perpendicular oriented lamellar domain over large areas was achieved using this method.

1.4 Summary

The self-assembly of block copolymers to form nanostructures is attractive since its ability to readily achieve nanoscale feature size over large areas is of interest in many research fields. These nanostructures can be made as nanodevices themselves, or act as templates for the fabrication of other functional materials. However, there is still a great deal of research to be done to make full use of this technique.

Although different methods to control orientation and improve the order within the block copolymer films have been described in this chapter, the application in advanced lithography is still limited by defects and lack of long-range order of the self-assembled morphology. Future work is still needed to create new block copolymer systems and patterning techniques to gain better control of the domain over the nanometer scale.

The continuous pursuit of the Moore's Law reveals our demand for even smaller feature size. But the lower size limit of the self-assembled structures is

limited by insufficient driving force to induce phase separation of smaller molecular weight block copolymer. Laser spike annealing[80], which has already been used to anneal photoresist materials to reduce the line edge roughness, may offer enough driving force since it can generates an extremely sharp temperature gradient.

Recently, some work has been reported to incorporate nanoparticles into the blocks and co-assembly with the polymer[81]. This method may create a hybrid system that contains both the advantages of block copolymers as well as the interesting mechanical and electrical properties of the nanoparticles. Works still need to be done to gain better control of the dispersion of nanoparticles within the polymer blocks.

Whether or not the block copolymer self-assembly technique will replace conventional UV lithography and be widely used in the semiconductor industry remains to be seen, but the fundamental research in this area will undoubtedly continue.

REFERENCE

1. Park, C., J. Yoon, and E.L. Thomas, *Enabling nanotechnology with self assembled block copolymer patterns.* Polymer, 2003. **44**(22), 6725-6760.
2. Krausch, G. and R. Magerle, *Nanostructured thin films via self-assembly of block copolymers.* Advanced Materials, 2002. **14**(21), 1579-+.
3. Lazzari, M. and M.A. Lopez-Quintela, *Block copolymers as a tool for nanomaterial fabrication.* Advanced Materials, 2003. **15**(19), 1583-1594.
4. Cheng, J.Y., et al., *Templated self-assembly of block copolymers: Top-down helps bottom-up.* Advanced Materials, 2006. **18**(19), 2505-2521.
5. Hawker, C.J. and T.P. Russell, *Block copolymer lithography: Merging "bottom-up" with "top-down" processes.* Mrs Bulletin, 2005. **30**(12), 952-966.
6. Li, M.Q., C.A. Coenjarts, and C.K. Ober, *Patternable block copolymers.* Block Copolymers Ii, 2005. **190**, 183-226.
7. Segalman, R.A., *Patterning with block copolymer thin films.* Materials Science & Engineering R-Reports, 2005. **48**(6), 191-226.
8. Li, M.Q. and C.K. Ober, *Block copolymer patterns and templates.* Materials Today, 2006. **9**(9), 30-39.
9. Stoykovich, M.P. and P.F. Nealey, *Block copolymers and conventional lithography.* Materials Today, 2006. **9**(9), 20-29.
10. Darling, S.B., *Directing the self-assembly of block copolymers.* Progress in Polymer Science, 2007. **32**(10), 1152-1204.
11. Bates, F.S. and G.H. Fredrickson, *Block copolymers - Designer soft materials.* Physics Today, 1999. **52**(2), 32-38.
12. Kim, H.C. and W.D. Hinsberg, *Surface patterns from block copolymer self-assembly.* Journal of Vacuum Science & Technology A, 2008. **26**(6), 1369-1382.
13. Krishnamoorthy, S., C. Hinderling, and H. Heinzelmann, *Nanoscale patterning with block copolymers.* Materials Today, 2006. **9**(9), 40-47.
14. Abetz, V. and P.F.W. Simon, *Phase behaviour and morphologies of block copolymers.* Block Copolymers I, 2005. **189**, 125-212.

15. van Zoelen, W. and G. ten Brinke, *Thin films of complexed block copolymers.* Soft Matter, 2009. **5**(8), 1568-1582.
16. Schift, H., *Nanoimprint lithography: An old story in modern times? A review.* Journal of Vacuum Science & Technology B, 2008. **26**(2), 458-480.
17. Hamley, I.W., *The physics of block copolymers*. Oxford science publications1998, Oxford ; New York: Oxford University Press. viii, 424 p.
18. Hashimoto, T., M. Shibayama, and H. Kawai, *Domain-Boundary Structure of Styrene-Isoprene Block Co-Polymer Films Cast from Solution .4. Molecular-Weight Dependence of Lamellar Microdomains.* Macromolecules, 1980. **13**(5), 1237-1247.
19. Leibler, L., *Theory of Microphase Separation in Block Co-Polymers.* Macromolecules, 1980. **13**(6), 1602-1617.
20. Ohta, T. and K. Kawasaki, *Equilibrium Morphology of Block Copolymer Melts.* Macromolecules, 1986. **19**(10), 2621-2632.
21. Bates, F.S. and G.H. Fredrickson, *Block Copolymer Thermodynamics - Theory and Experiment.* Annual Review of Physical Chemistry, 1990. **41**, 525-557.
22. Flory, P.J., *Principles of polymer chemistry*. The George Fisher Baker non-resident lectureship in chemistry at Cornell University1953, Ithaca,: Cornell University Press. 672 p.
23. Matsen, M.W. and F.S. Bates, *Unifying weak- and strong-segregation block copolymer theories.* Macromolecules, 1996. **29**(4), 1091-1098.
24. Hadjichristidis, N., M. Pitsikalis, and H. Iatrou, *Synthesis of block copolymers.* Block Copolymers I, 2005. **189**, 1-124.
25. Xu, T., et al., *The influence of molecular weight on nanoporous polymer films.* Polymer, 2001. **42**(21), 9091-9095.
26. Sivaniah, E., et al., *Symmetric diblock copolymer thin films on rough substrates: Microdomain periodicity in pure and blended films.* Macromolecules, 2008. **41**(7), 2584-2592.
27. Edrington, A.C., et al., *Polymer-based photonic crystals.* Advanced Materials, 2001. **13**(6), 421-425.

28. Russell, T.P., et al., *Characteristics of the Surface-Induced Orientation for Symmetric Diblock Ps/Pmma Copolymers.* Macromolecules, 1989. **22**(12), 4600-4606.
29. Coulon, G., et al., *Surface-Induced Orientation of Symmetric, Diblock Copolymers - a Secondary Ion Mass-Spectrometry Study.* Macromolecules, 1989. **22**(6), 2581-2589.
30. Green, P.F., T.M. Christensen, and T.P. Russell, *Ordering at Diblock Copolymer Surfaces.* Macromolecules, 1991. **24**(1), 252-255.
31. Mayes, A.M., et al., *Evolution of Order in Thin Block-Copolymer Films.* Macromolecules, 1994. **27**(3), 749-755.
32. Cai, Z.H., et al., *Experimental-Study of the Surface-Structure of Diblock Copolymer Films Using Microscopy and X-Ray-Scattering.* Journal of Chemical Physics, 1993. **98**(3), 2376-2386.
33. Coulon, G., et al., *Islands and Holes on the Free-Surface of Thin Diblock Copolymer Films .1. Characteristics of Formation and Growth.* Journal De Physique, 1990. **51**(24), 2801-2811.
34. Coulon, G., D. Ausserre, and T.P. Russell, *Interference Microscopy on Thin Diblock Copolymer Films.* Journal De Physique, 1990. **51**(8), 777-786.
35. Anastasiadis, S.H., et al., *The Morphology of Symmetric Diblock Copolymers as Revealed by Neutron Reflectivity.* Journal of Chemical Physics, 1990. **92**(9), 5677-5691.
36. Fasolka, M.J., et al., *Morphology of ultrathin supported diblock copolymer films: Theory and experiment.* Macromolecules, 2000. **33**(15), 5702-5712.
37. Fasolka, M.J., et al., *Observed substrate topography-mediated lateral patterning of diblock copolymer films.* Physical Review Letters, 1997. **79**(16), 3018-3021.
38. Morkved, T.L. and H.M. Jaeger, *Thickness-induced morphology changes in lamellar diblock copolymer ultrathin films.* Europhysics Letters, 1997. **40**(6), 643-648.
39. Morkved, T.L., et al., *Silicon nitride membrane substrates for the investigation of local structure in polymer thin films.* Polymer, 1998. **39**(16), 3871-3875.

40. Sakurai, S., et al., *Thermoreversible Morphology Transition between Spherical and Cylindrical Microdomains of Block-Copolymers.* Macromolecules, 1993. **26**(21), 5796-5802.
41. Kimishima, K., T. Koga, and T. Hashimoto, *Order-order phase transition between spherical and cylindrical microdomain structures of block copolymer. I. Mechanism of the transition.* Macromolecules, 2000. **33**(3), 968-977.
42. Hajduk, D.A., et al., *Observation of a Reversible Thermotropic Order-Order Transition in a Diblock Copolymer.* Macromolecules, 1994. **27**(2), 490-501.
43. Harrison, C., et al., *Mechanisms of ordering in striped patterns.* Science, 2000. **290**(5496), 1558-1560.
44. Harrison, C., et al., *Dynamics of pattern coarsening in a two-dimensional smectic system.* Physical Review E, 2002. **66**(1).
45. Harrison, C., et al., *Pattern coarsening in a 2D hexagonal system.* Europhysics Letters, 2004. **67**(5), 800-806.
46. Hammond, M.R., et al., *Temperature dependence of order, disorder, and defects in laterally confined diblock copolymer cylinder monolayers.* Macromolecules, 2005. **38**(15), 6575-6585.
47. Bodycomb, J., et al., *Single-grain lamellar microdomain from a diblock copolymer.* Macromolecules, 1999. **32**(6), 2075-2077.
48. Hashimoto, T., et al., *The effect of temperature gradient on the microdomain orientation of diblock copolymers undergoing an order-disorder transition.* Macromolecules, 1999. **32**(3), 952-954.
49. Mita, K., et al., *Cylindrical domains of block copolymers developed via ordering under moving temperature gradient.* Macromolecules, 2007. **40**(16), 5923-5933.
50. Mita, K., et al., *Ordering of cylindrical domains of block copolymers under moving temperature gradient: Separation of del T-induced ordering from surface-induced ordering.* Macromolecules, 2008. **41**(18), 6787-6792.
51. Berry, B.C., et al., *Orientational order in block copolymer films zone annealed below the order-disorder transition temperature.* Nano Letters, 2007. **7**(9), 2789-2794.

52. Yager, K.G., et al., *Disordered nanoparticle interfaces for directed self-assembly.* Soft Matter, 2009. **5**(3), 622-628.
53. Kim, G. and M. Libera, *Morphological development in solvent-cast polystyrene-polybutadiene-polystyrene (SBS) triblock copolymer thin films.* Macromolecules, 1998. **31**(8), 2569-2577.
54. Kim, G. and M. Libera, *Kinetic constraints on the development of surface microstructure in SBS thin films.* Macromolecules, 1998. **31**(8), 2670-2672.
55. Kim, S.H., M.J. Misner, and T.P. Russell, *Solvent-induced ordering in thin film diblock copolymer/homopolymer mixtures.* Advanced Materials, 2004. **16**(23-24), 2119-+.
56. Bosworth, J.K., et al., *Control of self-assembly of lithographically patternable block copolymer films.* Acs Nano, 2008. **2**(7), 1396-1402.
57. Bosworth, J.K., C.T. Black, and C.K. Obert, *Selective Area Control of Self-Assembled Pattern Architecture Using a Lithographically Patternable Block Copolymer.* Acs Nano, 2009. **3**(7), 1761-1766.
58. Paik, M.Y., et al., *Reversible Morphology Control in Block Copolymer Films via Solvent Vapor Processing: An in Situ GISAXS Study.* Macromolecules, 2010. **43**(9), 4253-4260.
59. Thurn-Albrecht, T., et al., *Ultrahigh-density nanowire arrays grown in self-assembled diblock copolymer templates.* Science, 2000. **290**(5499), 2126-2129.
60. Koppi, K.A., M. Tirrell, and F.S. Bates, *SHEAR-INDUCED ISOTROPIC-TO-LAMELLAR TRANSITION.* Physical Review Letters, 1993. **70**(10), 1449-1452.
61. Koppi, K.A., et al., *LAMELLAE ORIENTATION IN DYNAMICALLY SHEARED DIBLOCK COPOLYMER MELTS.* Journal De Physique Ii, 1992. **2**(11), 1941-1959.
62. Hamley, I.W., *The effect of shear on ordered block copolymer solutions.* Current Opinion in Colloid & Interface Science, 2000. **5**(5-6), 342-350.
63. Hamley, I.W. and V. Castelletto, *Small-angle scattering of block copolymers in the melt, solution and crystal states.* Progress in Polymer Science, 2004. **29**(9), 909-948.

64. Angelescu, D.E., et al., *Macroscopic orientation of block copolymer cylinders in single-layer films by shearing.* Advanced Materials, 2004. **16**(19), 1736-+.
65. Angelescu, D.E., et al., *Shear-induced alignment in thin films of spherical nanodomains.* Advanced Materials, 2005. **17**(15), 1878-+.
66. Vedrine, J., et al., *Large-area, ordered hexagonal arrays of nanoscale holes or dots from block copolymer templates.* Applied Physics Letters, 2007. **91**(14).
67. Marencic, A.P., et al., *Orientational order in sphere-forming block copolymer thin films aligned under shear.* Macromolecules, 2007. **40**(20), 7299-7305.
68. Sundrani, D., S.B. Darling, and S.J. Sibener, *Hierarchical assembly and compliance of aligned nanoscale polymer cylinders in confinement.* Langmuir, 2004. **20**(12), 5091-5099.
69. Sundrani, D., S.B. Darling, and S.J. Sibener, *Guiding polymers to perfection: Macroscopic alignment of nanoscale domains.* Nano Letters, 2004. **4**(2), 273-276.
70. Sundrani, D. and S.J. Sibener, *Spontaneous spatial alignment of polymer cylindrical nanodomains on silicon nitride gratings.* Macromolecules, 2002. **35**(22), 8531-8539.
71. Park, S.-M., et al., *Directed assembly of lamellae-forming block copolymers by using chemically and topographically patterned substrates.* Advanced Materials, 2007. **19**(4), 607-+.
72. Ruiz, R., et al., *Local defectivity control of 2D self-assembled block copolymer patterns.* Advanced Materials, 2007. **19**(16), 2157-+.
73. Park, S.-M., et al., *Observation of surface corrugation-induced alignment of lamellar microdomains in PS-b-PMMA thin films.* Soft Matter, 2009. **5**(5), 957-961.
74. Hong, S.W., et al., *Circular Nanopatterns over Large Areas from the Self-Assembly of Block Copolymers Guided by Shallow Trenches.* Acs Nano, 2011. **5**(4), 2855-2860.
75. Rockford, L., et al., *Polymers on nanoperiodic, heterogeneous surfaces.* Physical Review Letters, 1999. **82**(12), 2602-2605.

76. Ruiz, R., et al., *Density multiplication and improved lithography by directed block copolymer assembly.* Science, 2008. **321**(5891), 936-939.
77. Stoykovich, M.P., et al., *Directed assembly of block copolymer blends into nonregular device-oriented structures.* Science, 2005. **308**(5727), 1442-1446.
78. Liu, G., et al., *Morphology of lamellae-forming block copolymer films between two orthogonal chemically nanopatterned striped surfaces.* Physical Review Letters, 2012. **108**(6), 065502.
79. Kim, S.O., et al., *Epitaxial self-assembly of block copolymers on lithographically defined nanopatterned substrates.* Nature, 2003. **424**(6947), 411-414.
80. Sha, J., et al., *Submillisecond post-exposure bake of chemically amplified resists by CO2 laser spike annealing.* Journal of Vacuum Science & Technology B, 2009. **27**(6), 3020-3024.
81. Jang, S.G., et al., *Morphology Evolution of PS-b-P2VP Diblock Copolymers via Supramolecular Assembly of Hydroxylated Gold Nanoparticles.* Macromolecules, 2012. **45**(3), 1553-1561.

CHAPTER 2

CONTROL OF BLOCK COPOLYMER MICROSTRUCTURE THROUGH SOLVENT ANNEALING

2.1 Introduction

Block copolymers are known for their ability to self-assemble to form different microstructures[1-4]. In diblock copolymer systems, the microstructures can be spheres, cylinders, gyroids or lamellae depending on the volume fraction of one block relative to another[5]. These microstructures make block copolymers a promising template for many research areas involving controlled nanostructures[6-9].

One of the most promising applications is to use the self-assembled pattern of a block copolymer as a non-photochemical alternative means for next generation lithography[10-14]. Currently, high-resolution patterning with a goal of sub-20 nm dimensions is limited by the expensive optics of lithography tools[15, 16], while the self-assembly of block copolymer stands out with its ability to form microstructures with 5-50 nm feature size[17]. The size of the individual domains, as well as the domain spacing, can be controlled by simply changing the molecular weight and composition of a block copolymer[18-20]. With specially designed blocks, the block copolymer system can also fulfill various functionalities.

The diblock copolymer poly(α-methylstyrene)-*block*-poly(4-hydroxystyrene) (PαMS-*b*-PHOST) is a distinctive material since it can be patterned by both self-assembly techniques (bottom-up) and UV lithography (top-down)[21, 22]. The low entropy of mixing between the two blocks leads to a mesoscale morphology upon phase separation. Moreover, the low ceiling temperature of the PαMS blocks enables the selective removal of the PαMS microdomain and the PHOST blocks act as a chemically amplified photoresist when combined with photoacid generators and

cross-linkers. All these properties offer the PαMS-*b*-PHOST block copolymer system the ability to form a nanoporous etch mask that can be used to transfer the self-assembled pattern to an underlying substrate, a so called "combination of top-down and bottom-up patterning technique''.

However, controlling the microstructure of block copolymers is a key factor regarding its application in lithography. PαMS-*b*-PHOST with an overall molecular weight of 24 kg/mol and mass fraction of PαMS 29% forms disordered perpendicular cylinder morphology upon spin coating from propylene glycol methyl ether acetate (PGMEA) solution. For device application, an in-plane cylinder or sphere domain is required, so that achieving perpendicular orientation of microdomains needs a special treatment to gain the desired morphology as well as long-range order within the block copolymer films. As described in Chapter 1, the films can gain long-range order through thermal annealing[23, 24], solvent vapor annealing[25], application of electric fields[26], shear force[27, 28] and the use of chemically patterned substrates[29-31]. While thermal annealing is the most commonly used technique, PαMS-*b*-PHOST is not suitable for this method since PαMS has a lower decomposition temperature than its glass transition temperature, T_g. The block copolymer will degrade before reaching its T_g. Alternatively, solvent vapor annealing has been shown to control the spatial patterns in other polymer systems[32-35]. When the solvent vapor penetrates into the polymer film, the film will swell and give the polymer chains enough mobility to move around and reorient. This method decreases the T_g of the system and leads to phase separation.

Additionally, the selectivity of solvent for different blocks allows further control of the morphologies formed by the block copolymer film[36, 37].

Long-range order of the morphology is also necessary for patterning applications. Graphoepitaxy, or self-aligned self-assembly, is particularly interesting because the disordered polymer morphology can be confined and improved by a much larger feature created by conventional photolithography techniques[38-40]. This confinement can induce micron scale ordered regions in the film.

2.2 Experiments

2.2.1 Materials

PαMS-*b*-PHOST block copolymers (M_n=24 kg/mol, $f_{PαMS}$=29% and M_n=50 kg/mol, $f_{PαMS}$=34%) were synthesized as reported previously[22]. Polystyrene with a hydroxyl terminated end group (PS-OH, M_n=10 kg/mol, PDI=1.10) was obtained from Polymer Source and used as received. Tetrahydrofuran (THF), acetone and propylene glycol methyl ether acetate (PGMEA) were purchased from Fisher Scientific and used as received. Single-polished <100> silicon wafers containing a ~2nm native oxide layer were obtained from WRS.

2.2.2 Film Preparation

Silicon wafers were cleaned by oxygen plasma using PT72 reactive ion etcher for 5 min at 150w, 100 mTorr and 50 sccm oxygen. Solutions of 1wt% PS-OH in methyl isobutyl keytone (MIBK) were spin-coated onto the clean wafers (1500 rpm,

60s, 500 r/sec^2). Then the wafers were pre-baked at 90 °C for 60s and baked in a vacuum oven for 12 hours at 140 °C. Excess polystyrene was washed away by soaking in toluene for 2 minutes and the wafer was blown dry by stream of nitrogen. PαMS-*b*-PHOST was dissolved in PGMEA (1 wt% for M_n=24 kg/mol and 2 wt% for M_n=50 kg/mol) and spin-coated on top of the polystyrene brush layer (2000 rpm, 60s, 400 r/sec^2). The wafers were then cut into 20 mm× 20 mm pieces to prepare samples for solvent annealing.

The solvent vapor annealing was performed in a 1L desiccator or using the specially designed flow chamber (Figure 6.1)[41]. The amount of solvent and time used for solvent annealing varied case by case.

2.2.3 Trench preparation

Topographic features on silicon wafers were created by conventional photolithography to help align the block copolymer via geographoepitaxy. Silicon wafers coated with photoresists were first exposed to a DUV pattern and then a dry etched to create a series of 70 nm deep patterns on the silicon wafers. Lastly, the photoresists were stripped in an oxygen plasma. Further details can be found in section 2.3.3.a

2.2.4 Characterization

After solvent annealing, the samples were characterized by atomic force microscopy (AFM) using either Veeco Dimension 3100 at the Cornell Nanobiotechnology Center (NBTC) or a Veeco Icon at the Cornell Nanoscale Facility

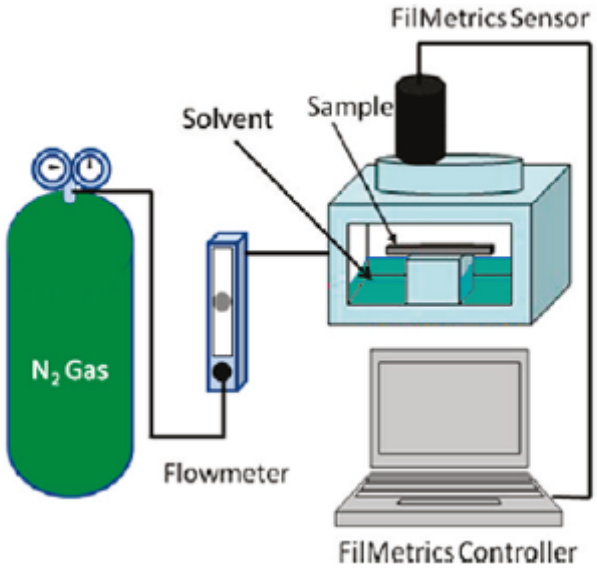

Figure 2.1 Schematic of the flowing chamber equipment for solvent vapor annealing.

(Adapted from ref 41. Copyright 2010 American Chemical Society.)

(CNF). The film thickness was measured using a Filmetrics F20 and Profilometer P10 at CNF.

2.3 Results and Discussion

2.3.1 Solvent vapor annealing

It has been reported by others that solvent vapor annealing is an effective method with its ability to tune the microstructure of a block copolymer. When solvent vapor enters the block copolymer film, it will fully or partially swell the polymer chains and give them enough mobility to move and reorient. We observe parallel cylinder domain orientation when polymer chains gain mobility due to swelling in THF (Figure 2.2 b), a good solvent for both polymer blocks. In this case, preferential surface wetting by the PHOST block drives parallel domain orientation. The block copolymer used here has a molecular weight of 24 kg/mol and contains 29% PαMS blocks and lies in the cylinder region of the phase diagram (Figure 2.2 a). The diameter of the cylinders was 18 nm and the center-to-center distance was 22 nm as measured by AFM. The film thickness is 28 nm measured by filmetrics. The same morphology can be obtained using a higher molecular weight block copolymer (M_n=50 kg/mol) containing 34% PαMS blocks as this composition also falls into the region of the cylinder morphology on the phase diagram.

A unique advantage of solvent annealing over other methods is its ability to control the block copolymer microstructure through choice of solvent. We find that using the same block copolymer and annealing in acetone vapor gives spherical

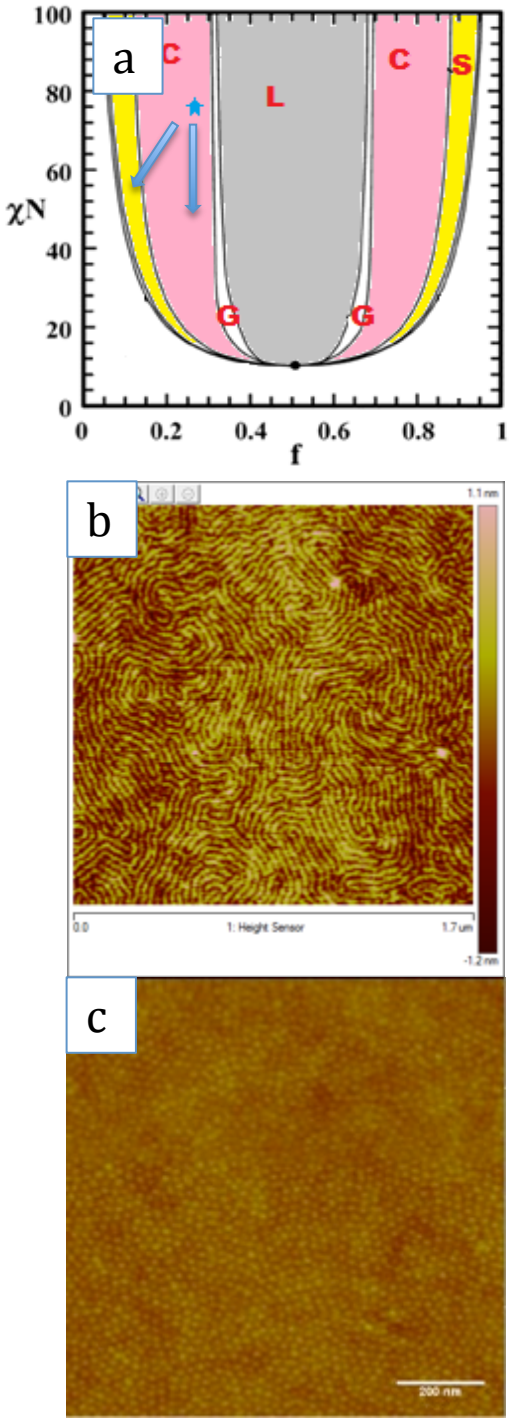

Figure 2.2 a) Schematic phase diagram of PαMS-*b*-PHOST. b) AFM height image of PαMS-*b*-PHOST after THF annealing. c) AFM height image of PαMS-*b*-PHOST after acetone annealing

morphology (Figure 2.2 c). Acetone is not a good solvent for PαMS blocks, though it is a good solvent for the PHOST homopolymer. Consequently, acetone preferentially swells the PHOST block in the swollen state and induces an order-order transition from cylindrical to spherical morphology. The resulting morphology may be kinetically trapped in the dry state when the solvents in the films have completely evaporated. It is difficult to distinguish between perpendicular cylinder morphology and a sphere phase by looking at the AFM image alone. However, it had been shown by a former group member using grazing incidence small-angle X-ray scattering (GISAXS) that the morphology after acetone annealing is actually sphere[36]. We can also get the same spherical morphology using a higher molecular weight block copolymer.

2.3.2 Solvent annealing technique

Traditionally, the solvent annealing is carried out in a glass desiccator or a sealed jar with a certain amount of solvent placed in a small petri dish cover at the bottom of the chamber. In this setup, there are only two parameters we can control, the amount of solvent and the annealing (6 ml and 5.5 h for acetone annealing, 4 ml and 9 h for THF annealing). However, the temperature and pressure also affect the annealing process but these are not controlled. In order to gain better control over the film during the solvent vapor annealing, a former group member designed and used a special flow chamber (Figure 2.1)[41]. An in-situ GISAXS study of the solvent vapor annealing process revealed that the film must swell to a certain thickness in order for the polymer chains to phase separate and reorient. The thickness of the

film, measured by a filmetrics sensor, can be controlled by adjusting the amount of solvent vapor inside the chamber through adjusting the nitrogen flow. The smaller the nitrogen flow, the more solvent inside the chamber which leads to an increase in film thickness.

However, in these experiments a much smaller molecular weight block copolymer was used, which forms a film that is too thin to be measured by GISAXS. So we tried different swelling ratios and measured the film surface using AFM in order to find the right conditions to obtain the desired morphology. Moreover, since the film is too thin (30-60 nm), it is easy for it to become unstable and form holes and islands (dewetting) if we increase the film thickness too quickly. The best way is to let the film stabilize for 15 min after changing the nitrogen flow, giving the polymer chains enough time to reorient. Figure 2.3 a shows an example of THF annealing using the flow chamber. As we can see from the figure, the initial film thickness is 30.2 nm and when we inject the solvent into the chamber the film thickness increases immediately. The flow meter is kept at full flow rate for the first five minutes and then is decreased every fifteen minutes to enable the solvent to swell the polymer film. When the thickness reaches the target swelling ratio (~160%), it is important to carefully adjust the flow meter a little bit to keep the thickness constant for at least 20 minutes. After that, a rapid evaporation of the solvent is achieved by opening the chamber directly to trap the morphology into the dry state.

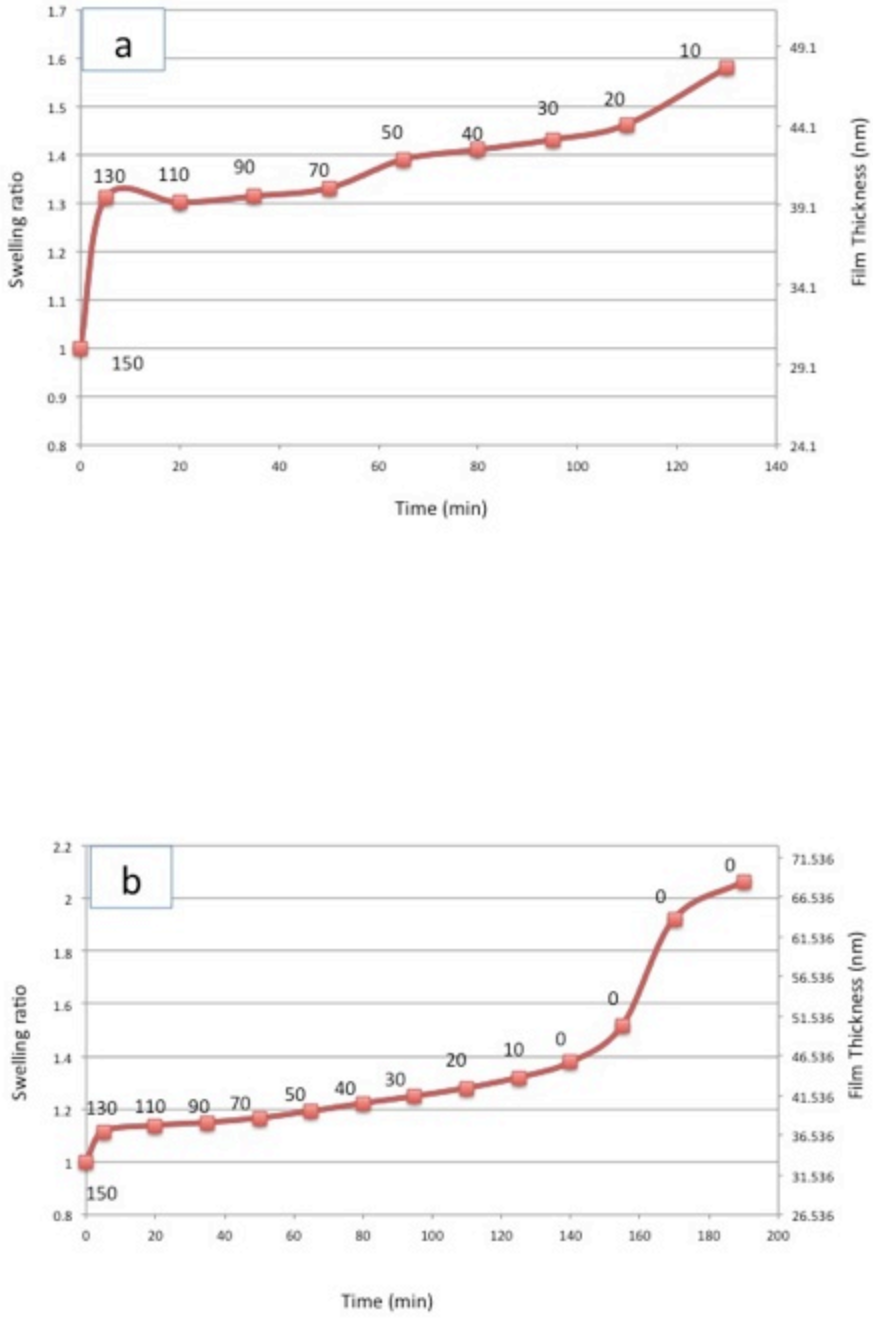

Figure 2.3 Time vs. thickness profile and swelling ratio of a) THF and b) acetone annealing. The number on the curve indicates the value on the flow meter

An example of thickness profile vs. time for acetone annealing is shown is Figure 2.3 b. A swelling ratio of 205 % is required to allow the spherical morphology to form. It is the same trend as the THF annealing except for a longer annealing time since acetone is a good solvent for PHOST blocks but not good for the PαMS blocks. Besides, as we can see from the figure, the film thickness is still below the target value when we set the flow meter to zero. A further increase of the film thickness can be achieved by blocking the other end of the chamber to increase the amount of solvent inside the chamber.

2.3.3 Graphoepitaxy

High-resolution lithography applications will require both polymer domain registration and ordering within the self-assembled block copolymer film. In our experiments we prepared 70 nm deep trenches on silicon wafer by conventional UV lithography and etching techniques to help align the polymer.

First, an anti-reflective coating (ARC3) was spin-coated onto the silicon wafer (4500 rpm, 45s) and baked at 185 °C for 90s. Then, the photoresist UV210 was spin-coated on top of the ARC3 layer (4250 rpm, 60s) and baked at 135 °C for 60s. Exposure step was carried out on the ASML 300C DUV Stepper (245nm, 25 mJ/cm^2). A post-exposure bake at 115 °C for 90s is needed. After that, the wafer was developed using a Hamatech-Steag wafer processor (MIF 726 for 60s). Profilometer gave a thickness of 400 nm for the resist layer and 100 nm for the ARC3 layer. Then an argon/oxygen etch was performed to etch away the ARC3 layer using Oxford 81 etcher (42.5 sccm Ar, 7.5 sccm O_2, 15 mTorr, 75 W, 120 s). The wafer was tested

again on profilometer to maker sure no ARC3 layer was left. A sequential etching steps on the PT72 etcher was performed to created trenches on silicon wafer. First, a 12 min CF_4 etch (30 sccm CF_4, 50w, 40 mTorr) was performed to get a 70 nm deep trenches, and a 5 min oxygen plasma etch was followed to remove all the photoresist and create hydroxyl end group on the silicon wafer for bonding with the PS-OH brush.

The surface functionalization of the substrate with PS-OH brush is also a crucial factor to get long-range order of the polymer domain[42]. A dehydration process happens between the hydroxyl end group on the polystyrene brush and the silicon wafer during an overnight baking at 140 °C, and leaves a thin layer (~5 nm) of PS brush prior to PαMS-*b*-PHOST deposition in order to achieve preferential wetting by the PαMS minority block to avoid pinning effects. The same solution and spin speed for the 24 kg/mol block copolymer were used here. We observed registration of parallel-oriented cylinder domains upon THF annealing (Figure 2.4 a), while films deposited on untreated substrate do not self-align to the patterned substrate upon THF annealing (Figure 2.4 b). Solvent annealing in acetone rather than THF results in aligned hexagonal arrays of dots (Figure 2.4 c). We have achieved an almost defect-free domain alignment of parallel cylinder (figure 2.5 a) or spheres (Figure 2.5 b) within micro scale images. Patterns were consistent over all areas of the wafer.

2.3.4 Selective removal of the PαMS blocks

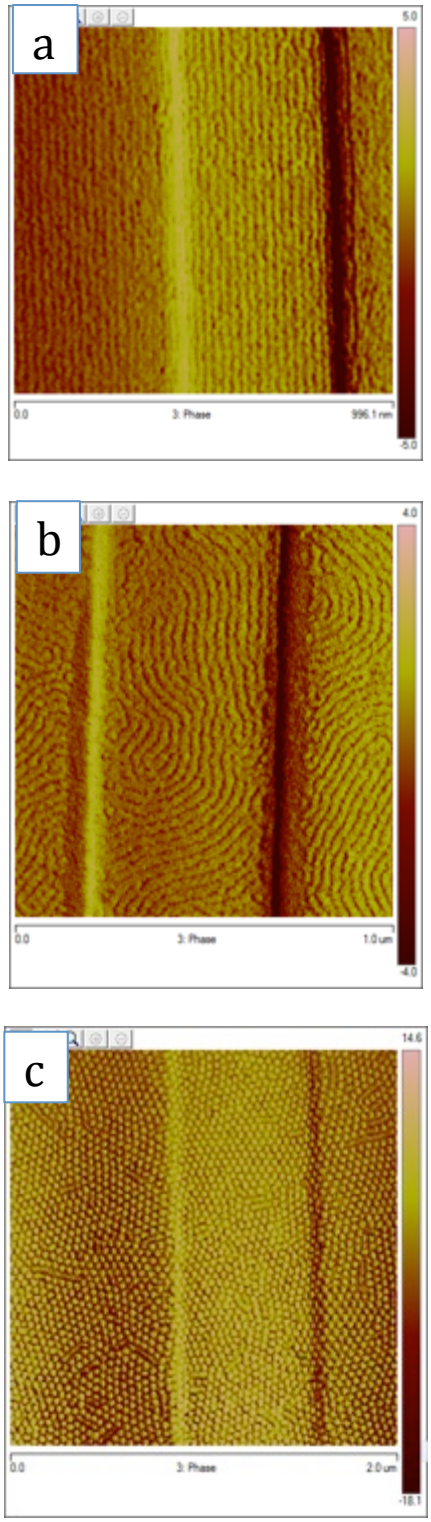

Figure 2.4 AFM phase image of a) parallel cyinder in a PS-OH treated silicon trench, b) random cylinders on un-treated substrate and c) ordered sphere morphology.

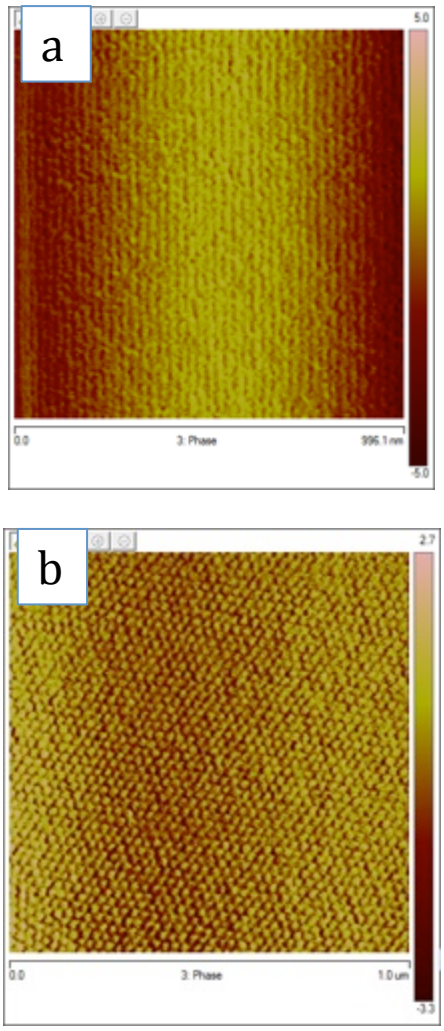

Figure 2.5 AFM phase images of the block copolymer films annealed in a) THF and b) acetone with also defect-free morphology in micro scale.

One of the most important features of the PαMS-*b*-PHOST block copolymer system is the ability to selectively remove the PαMS domain to create a nanoporous etch mask with potential for device fabrication. The reason for this is the low ceiling temperature of PαMS (T_c~65 °C), above which the polymer thermodynamically prefers to exist as monomers[43], so it is generally impossible to polymerize the α-methyl styrene above its T_c. In this experiment we used an UV/Ozone cleaner to selectively remove the PαMS domain. The sample film with cylinder morphology (Figure 2.6 a) was heated at 80 °C while exposing the block copolymer to vacuum ultraviolet radiation and an oxygen-rich environment. The temperature is enough to bring the α-methyl styrene above its T_c, while the atomic oxygen, which formed by UV radiation of oxygen molecules, reacts with the polymer to form free radicals that accelerate the degradation of PαMS. The byproducts are carbon dioxide and water vapor, which are purged from the chamber. A simple soak in ethanol afterwards was performed to effectively remove the degraded α-methyl styrene oligomers.

The etch rate of the PαMS domain is about twice of the PHOST domain (10 nm/ min and 5 nm/min for PαMS and PHOST, respectively). AFM amplitude images as well as cross-section contrast profiles after UV/Ozone treatment are shown in Figure 2.6 b. We can see that the contrast between the two domains has been greatly improved.

2.4 Conclusions

We have demonstrated here the ability to control the microstructure as well as the domain registration using the PαMS-*b*-PHOST diblock copolymer system.

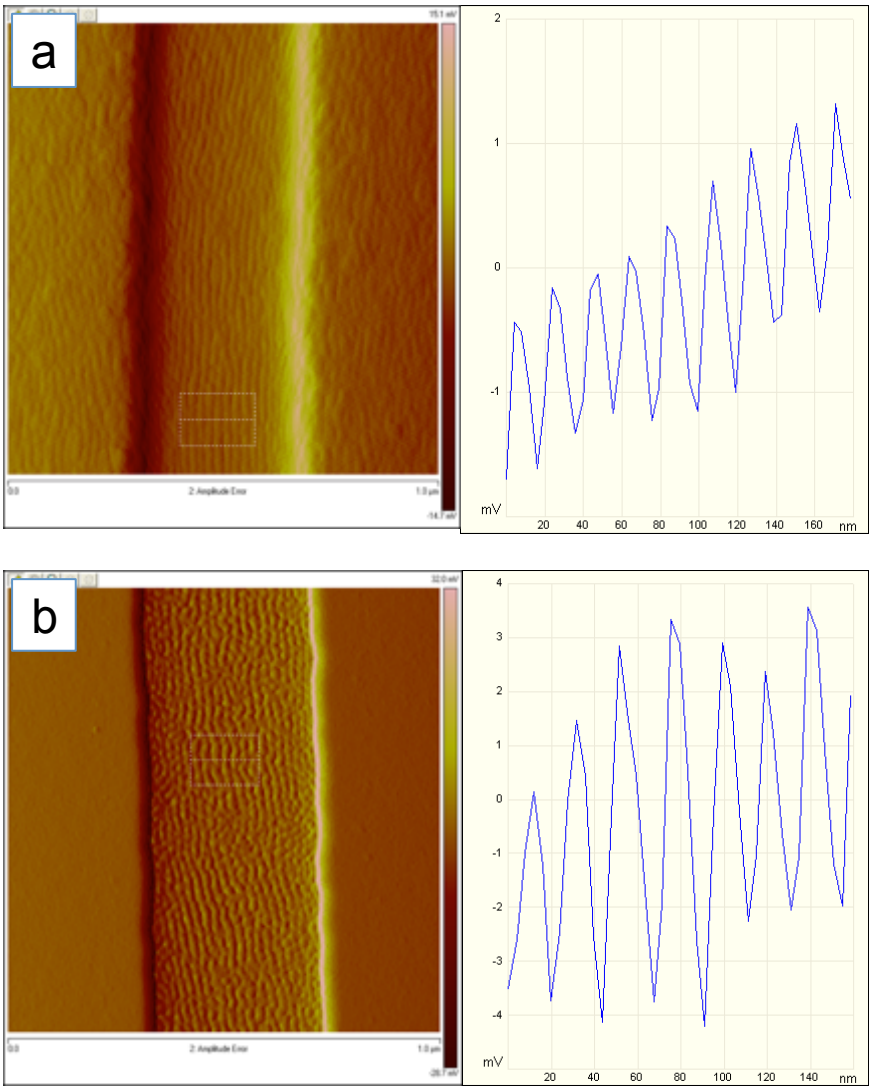

Figure 2.6 AFM amplitude images of the block copolymer a) before and b) after 4 min UV/Ozone treatment. The images on the right show the cross-section contrast profile of the selected area.

Different microstructures can be achieved by annealing the block copolymer films in selective solvent vapors. Aligning the morphology within trenches helps the film to gain long-range order and domain registration. In addition, one of the domains can be selectively removed to create a nanoporous etch mask to allow thansfer of the self-assembled pattern to the substrate. This combination of lithographic patterning and self-assembly of block copolymer processes suggests a possible new method for future device fabrication.

2.5 Acknowledgements

This work was supported by the National Science Foundation. The author would like to thank Evan Schwartz and Joan K. Bosworth for their help and advice with the project, Carol Newby for the help with the lithography patterning steps, Hee-Soo Yoo for synthesis the block copolymer and Michelle Chavis for the help with the solvent annealing chamber. This work was performed using facilities at the Cornell NanoScale Facility (CNF), a member of the National Nanotechnology Infrastructure Network, which is supported by the National Science Foundation (Grant ECS-03335765). This work also made use of the facilities of the Cornell Nanobiotechnology Center (NBTC).

REFERENCES

1. Hashimoto, T., M. Shibayama, and H. Kawai, *Domain-Boundary Structure of Styrene-Isoprene Block Co-Polymer Films Cast from Solution .4. Molecular-Weight Dependence of Lamellar Microdomains.* Macromolecules, 1980. **13**(5), 1237-1247.
2. Leibler, L., *Theory of Microphase Separation in Block Co-Polymers.* Macromolecules, 1980. **13**(6), 1602-1617.
3. Ohta, T. and K. Kawasaki, *Equilibrium Morphology of Block Copolymer Melts.* Macromolecules, 1986. **19**(10), 2621-2632.
4. Bates, F.S. and G.H. Fredrickson, *Block Copolymer Thermodynamics - Theory and Experiment.* Annual Review of Physical Chemistry, 1990. **41**, 525-557.
5. Bates, F.S. and G.H. Fredrickson, *Block copolymers - Designer soft materials.* Physics Today, 1999. **52**(2), 32-38.
6. Kim, H.C. and W.D. Hinsberg, *Surface patterns from block copolymer self-assembly.* Journal of Vacuum Science & Technology A, 2008. **26**(6), 1369-1382.
7. Krausch, G. and R. Magerle, *Nanostructured thin films via self-assembly of block copolymers.* Advanced Materials, 2002. **14**(21), 1579-+.
8. Li, M.Q. and C.K. Ober, *Block copolymer patterns and templates.* Materials Today, 2006. **9**(9), 30-39.
9. Park, C., J. Yoon, and E.L. Thomas, *Enabling nanotechnology with self assembled block copolymer patterns (vol 44, pg 6725, 2003).* Polymer, 2003. **44**(25), 7779-7779.
10. Park, M., et al., *Block copolymer lithography: Periodic arrays of similar to 10(11) holes in 1 square centimeter.* Science, 1997. **276**(5317), 1401-1404.
11. Hawker, C.J. and T.P. Russell, *Block copolymer lithography: Merging "bottom-up" with "top-down" processes.* Mrs Bulletin, 2005. **30**(12), 952-966.
12. Cheng, J.Y., et al., *Templated self-assembly of block copolymers: Top-down helps bottom-up.* Advanced Materials, 2006. **18**(19), 2505-2521.

13. Kim, H.C., S.M. Park, and W.D. Hinsberg, *Block Copolymer Based Nanostructures: Materials, Processes, and Applications to Electronics.* Chemical Reviews, 2010. **110**(1), 146-177.
14. Bang, J., et al., *Block Copolymer Nanolithography: Translation of Molecular Level Control to Nanoscale Patterns.* Advanced Materials, 2009. **21**(47), 4769-4792.
15. Rothemund, P.W.K., *Folding DNA to create nanoscale shapes and patterns.* Nature, 2006. **440**(7082), 297-302.
16. Wua, B. and A. Kumar, *Extreme ultraviolet lithography: A review.* Journal of Vacuum Science & Technology B, 2007. **25**(6), 1743-1761.
17. Edrington, A.C., et al., *Polymer-based photonic crystals.* Advanced Materials, 2001. **13**(6), 421-425.
18. Matsen, M.W. and F.S. Bates, *Unifying weak- and strong-segregation block copolymer theories.* Macromolecules, 1996. **29**(4), 1091-1098.
19. Xu, T., et al., *The influence of molecular weight on nanoporous polymer films.* Polymer, 2001. **42**(21), 9091-9095.
20. Hadjichristidis, N., M. Pitsikalis, and H. Iatrou, *Synthesis of block copolymers.* Block Copolymers I, 2005. **189**, 1-124.
21. Du, P., et al., *Additive-driven phase-selective chemistry in block copolymer thin films: The convergence of top-down and bottom-up approaches.* Advanced Materials, 2004. **16**(12), 953-+.
22. Li, M.Q., et al., *Spatially controlled fabrication of nanoporous block copolymers.* Chemistry of Materials, 2004. **16**(20), 3800-3808.
23. Hajduk, D.A., et al., *Observation of a Reversible Thermotropic Order-Order Transition in a Diblock Copolymer.* Macromolecules, 1994. **27**(2), 490-501.
24. Harrison, C., et al., *Mechanisms of ordering in striped patterns.* Science, 2000. **290**(5496), 1558-1560.
25. Mori, K., H. Hasegawa, and T. Hashimoto, *Ordered Structure in Block Polymer-Solutions .6. Possible Nonequilibrium Effects on Growth of Self-Assembling Structures.* Polymer, 1990. **31**(12), 2368-2376.

26. Thurn-Albrecht, T., et al., *Ultrahigh-density nanowire arrays grown in self-assembled diblock copolymer templates.* Science, 2000. **290**(5499), 2126-2129.
27. Angelescu, D.E., et al., *Macroscopic orientation of block copolymer cylinders in single-layer films by shearing.* Advanced Materials, 2004. **16**(19), 1736-+.
28. Angelescu, D.E., et al., *Shear-induced alignment in thin films of spherical nanodomains.* Advanced Materials, 2005. **17**(15), 1878-+.
29. Kim, S.O., et al., *Epitaxial self-assembly of block copolymers on lithographically defined nanopatterned substrates.* Nature, 2003. **424**(6947), 411-414.
30. Stoykovich, M.P., et al., *Directed assembly of block copolymer blends into nonregular device-oriented structures.* Science, 2005. **308**(5727), 1442-1446.
31. Ruiz, R., et al., *Density multiplication and improved lithography by directed block copolymer assembly.* Science, 2008. **321**(5891), 936-939.
32. Fukunaga, K., et al., *Large-scale alignment of ABC block copolymer microdomains via solvent vapor treatment.* Macromolecules, 2000. **33**(3), 947-953.
33. Cavicchi, K.A., K.J. Berthiaume, and T.P. Russell, *Solvent annealing thin films of poly(isoprene-b-lactide).* Polymer, 2005. **46**(25), 11635-11639.
34. Tokarev, I., et al., *Microphase separation in thin films of poly(styrene-block-4-vinylpyridine) copolymer-2-(4 '-hydroxybenzeneazo)benzoic acid assembly.* Macromolecules, 2005. **38**(2), 507-516.
35. Jung, Y.S., et al., *A Path to Ultranarrow Patterns Using Self-Assembled Lithography.* Nano Letters, 2010. **10**(3), 1000-1005.
36. Bosworth, J.K., et al., *Control of self-assembly of lithographically patternable block copolymer films.* Acs Nano, 2008. **2**(7), 1396-1402.
37. Jung, Y.S. and C.A. Ross, *Solvent-Vapor-Induced Tunability of Self-Assembled Block Copolymer Patterns.* Advanced Materials, 2009. **21**(24), 2540-+.
38. Sundrani, D. and S.J. Sibener, *Spontaneous spatial alignment of polymer cylindrical nanodomains on silicon nitride gratings.* Macromolecules, 2002. **35**(22), 8531-8539.

39. Sundrani, D., S.B. Darling, and S.J. Sibener, *Guiding polymers to perfection: Macroscopic alignment of nanoscale domains.* Nano Letters, 2004. **4**(2), 273-276.
40. Sundrani, D., S.B. Darling, and S.J. Sibener, *Hierarchical assembly and compliance of aligned nanoscale polymer cylinders in confinement.* Langmuir, 2004. **20**(12), 5091-5099.
41. Paik, M.Y., et al., *Reversible Morphology Control in Block Copolymer Films via Solvent Vapor Processing: An in Situ GISAXS Study.* Macromolecules, 2010. **43**(9), 4253-4260.
42. Harrison, C., et al., *Reducing substrate pinning of block copolymer microdomains with a buffer layer of polymer brushes.* Macromolecules, 2000. **33**(3), 857-865.
43. Cowie, J.M. and S. Bywater, *Molecular Weight Distribution Changes during Thermal Breakdown of Poly-Alpha-Methylstyrene.* Journal of Polymer Science, 1961. **54**(159), 221-&.

CHAPTER 3

PATTERNING MULTIPLE BLOCK COPOLYMERS USING ORTHOGONAL PROCESSING

3.1 Introduction

We have demonstrated the ability of block copolymer to self-assemble to form controlled microstructures. The use of these microstructures for patterning holds much promise as an alternative for high-resolution lithography of future microelectronic devices[1]. However, this approach is limited by the ability of selective-area patterning of more than one self-assembled morphology of several block copolymers within a single layer. There have been several reports showing control of two domain orientations with a single-phase morphology or even two morphologies within a block copolymer. For example, surface-neutralizing techniques have been used extensively in patterning poly (styrene-*block*-methyl methacrylate) (PS-*b*-PMMA) to gain both perpendicular and parallel orientations of cylindrical or lamellar morphology[2-8]. Our former group members have developed a "lock and switch" technique in which the block copolymer can be selectively cross-linked when adding photoacid generator (PAG) and cross-linkers and exposing the combination to UV light[9]. The unexposed block copolymer film can be re-annealed in another solvent to switch to a different morphology while the cross-linked areas retain their original morphology. However, such methods are still limited by using only one block copolymer to achieve the desired results. Patterning of block copolymers with different compositions or chemistries, which offers much more versatile control of the self-assembled patterns, is traditionally not applicable due to damage and intermixing caused by the spin coating of a second polymer solution on top of the first polymer film.

A new technique has been developed in our group that may solve the intermixing problem of patterning multiple polymers by using a fluorinated photoresist and solvent system[10-12]. The fluorinated materials and solvents are typically immiscible with organic solvents and water, and are used to form overlaying stacks in functional organic electronic devices with excellent performance and stability[13, 14]. By substituting the traditional photoresist with fluorinated photoresist, which can also be patterned by conventional UV lithography, the underlining block copolymer can retain its morphology as there is little or no intermixing between the resist and the polymer layers. In addition, the developing and stripping solvents used here do not harm the block copolymer layer. We term this "orthogonal processing" and the concept allows for deposition of multiple block copolymers, with different sizes and pitches, adjacent to each other on the same layer.

At the end of the last chapter, we also demonstrated the ability to control the alignment and long-range order within the polymer films by creating trench features on the substrates prior to the deposition of block copolymers. This method can be combined with orthogonal processing techniques to create ordered microdomains with different morphologies within a single polymer layer. Due to the ability to selectively remove one block of the block copolymer[15], the self-assembled pattern can be further transferred to the silicon substrate by a short etch step to create paths for semiconductor device fabrication. This orthogonal patterning process may also be applicable to other functional polymer systems.

3.2 Experiments

3.2.1 Materials

PαMS-*b*-PHOST block copolymers (M_n=24 kg/mol, $f_{PαMS}$=29% and M_n=50 kg/mol, $f_{PαMS}$=34%) were synthesized as reported previously[15]. Polystyrene with a hydroxyl terminated end group (PS-OH, M_n=10 kg/mol, PDI=1.10) was obtained from Polymer Source and used as received. Triphenyl sulfonium triflate (TPST) photoacid generator was obtained from Aldrich and used as received. Tetramethoxymethylglycouril (TMMGU, "powderlink 1174") was donated by Cytec Industries. The fluorinated photoresist (OSCoR 2312) and hydrofluoroether (HFE) solvents (Ortho Stripper 700 and Ortho developer 100) were obtained from Orthogonal Inc. Tetrahydrofuran (THF), acetone and propylene glycol methyl ether acetate (PGMEA) were purchased from Fisher Scientific and used as received. Single-polished <100> silicon wafers containing a ~2nm native oxide layer were obtained from WRS.

3.2.2 Film Preparation

Silicon wafers with trenches were prepared by conventional photolithography methods as described in chapter 2. PS-OH brushes were spin-coated on to the wafers and baked overnight. Block copolymer PαMS-*b*-PHOST dissolved in PGMEA (1 wt% for M_n=24 kg/mol and 2 wt% for M_n=50 kg/mol) was mixed with 1.5 wt.% TPST photoacid generator and 4 wt.% TMMGU cross-linker relative to the weight of the polymer. Polymers with lower molecular weights

(M_n=24 kg/mol) were spin-coated on top of the polystyrene layer and solvent annealed in the flow chamber as described in last chapter also[16].

After solvent annealing, the block copolymer was exposed to 254 nm UV light (dose=360 mJ/cm^2) for 10 min and baked at 115 °C for 60 s to accelerate the acid catalyzed crosslinking reaction.

3.2.3 Deposition and Patterning of the Orthogonal Photoresist

OSCoR 2312 photoresist was spin-coated on top of the cross-linked block copolymer film (2000 rpm, 60s, 400 r/sec^2) to yield a thickness of 1000 nm. The sample was pre-baked at 115 °C for 60 s and exposed to 365 nm UV radiation using an ABM Contact Aligner for 20 s. After exposure the film was baked at 115 °C to accelerate the acid diffusion and developed in Ortho 700 for 120 s to remove the unexposed photoresists. Oxygen plasma etching was performed using an Oxford 81 Etcher for 30 s to etch through the first block copolymer film while also etching the top few hundreds nanometers of the photoresist. HMDS priming treatment of the exposed photoresist pattern was performed in a Yield Engineering Systems (YES-LPIII) vacuum oven.

3.2.4 Deposition of the second block copolymer film

PS-OH brush dissolved in cyclohexane (0.5 wt.%) was spin-coated on top of the silicon wafer and baked at 90 °C for 60s. Excess brush was washed away in cyclohexane for 120 s and a higher molecular weight block copolymer (M_n=50

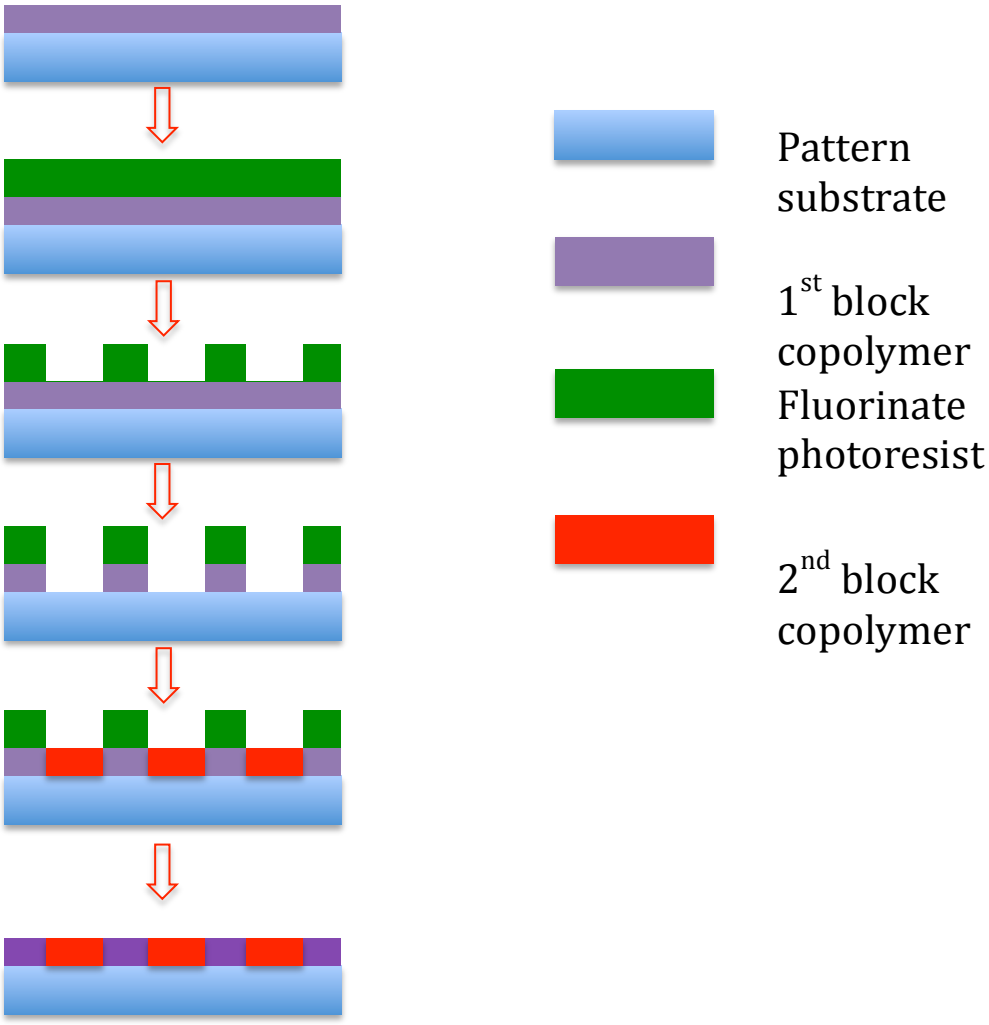

Figure 3.1 Schematic of the orthogonal patterning process

kg/mol) was spin-coated on the wafer. Then the photoresist was stripped away in Orthogonal 100 Stripper for 10 minutes. Solvent annealing followed by a UV irradiation was performed to achieve the morphology within the second block copolymer film.

3.2.5 Characterization

After solvent annealing, the samples were characterized by atomic force microscopy (AFM) using either Veeco Dimension 3100 at Cornell Nanobiotechnology Center (NBTC) or Veeco Icon at Cornell Nanoscale Facility (CNF). The film thickness was measured by Filmetrics F20 and Profilometer P10 at CNF.

3.3 Results and Discussions

A schematic drawing of the process flow is shown in Figure 3.1.

3.3.1 Solvent annealing and crosslinking of the first block copolymer film

The orthogonal patterning process requires two independent solvent annealing steps and there are two potential challenges to achieve a good result: 1) the first block copolymer film may be damaged by the solution used when depositing the second block copolymer and 2) the first block copolymer region will also swell during the solvent annealing process of the second block copolymer and thus the morphology of the first block copolymer will be lost. To solve the first problem, we can apply a layer of fluorinated materials to avoid the intermixing

between the different polymer layers. And the second problem can be solved by "locking" in the morphology of the first block copolymer film by using a UV crosslinking technique[15].

The PHOST blocks are designed as a negative-tone photoresist when combined with TPST as photoacid generator (PAG) and TMMGU as cross-linker[17-19]. The detailed crosslinking reaction is shown in Figure 3.2. In general, exposure to 248 nm UV radiation triggers the acid generation of the PAG, which will attack the oxygen atom of the methoxy group of the TMMGU. The formation of a carbocation will further attack the hydroxyl group of PHOST to complete the crosslinking process. This crosslinking chemistry only takes place in the PHOST matrix, but it can successfully lock the morphology within the polymer film, which will not change upon annealing in another solvent vapor. What It is also important in this method is to add a small enough amount of PAG and cross-linker such that they do not affect the self-assembly behavior of the block copolymer. The same cylindrical (Figure 3.3 a) and spherical (Figure 3.3 b) morphologies were successfully achieved using block copolymers contain PAG and cross-linker with the same solvent annealing conditions described in the last chapter. Figure 3.4 c shows that a block copolymer first annealed in acetone solvent vapor and then in THF solvent vapor remains in the spherical morphology, proving that the crosslinking reaction of the PHOST matrix was successful.

3.3.2 Subtractive patterning of the first block copolymer

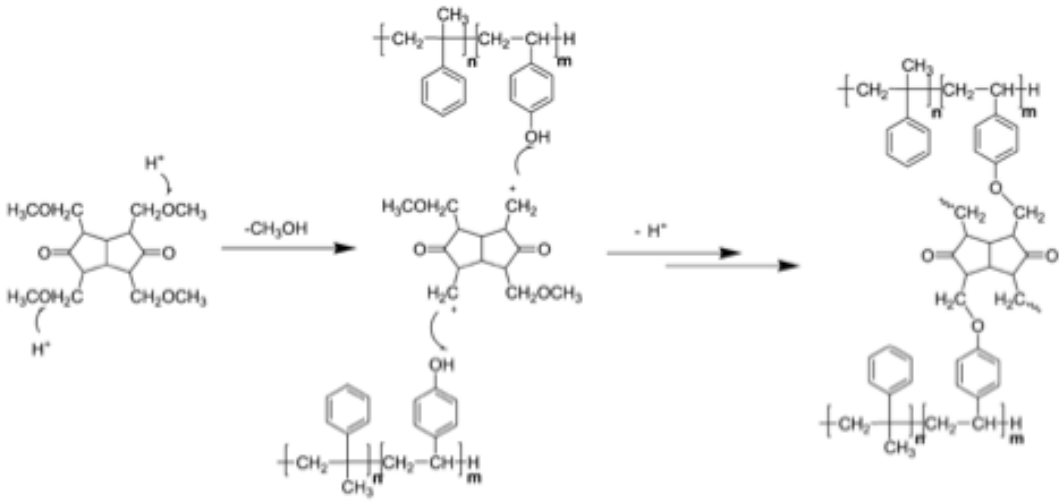

Figure 3.2 Proposed cross-linking mechanism of the PHOST blocks

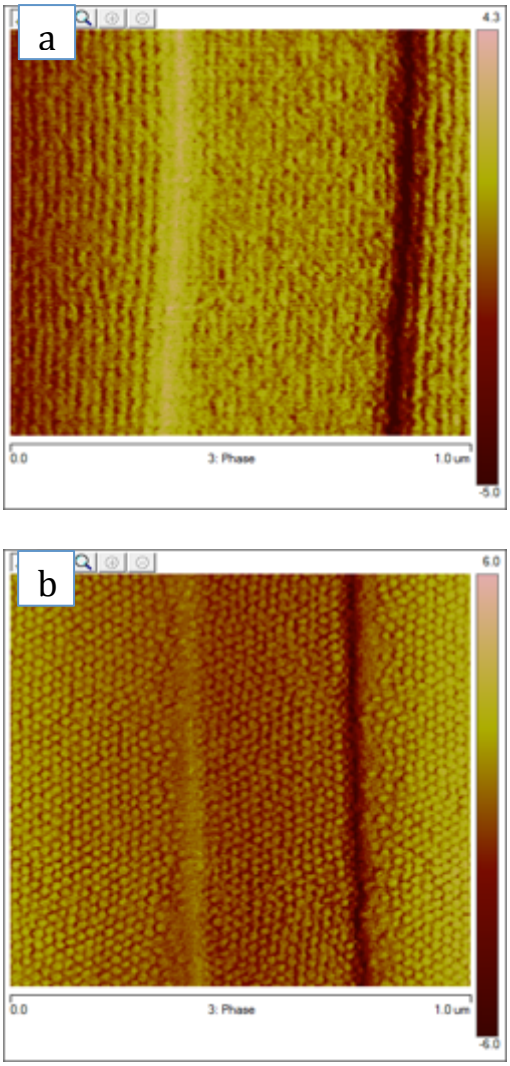

Figure 3.3 AFM phase images of the block copolymers containing PAG and cross-linkers after annealing in a) THF and b)acetone

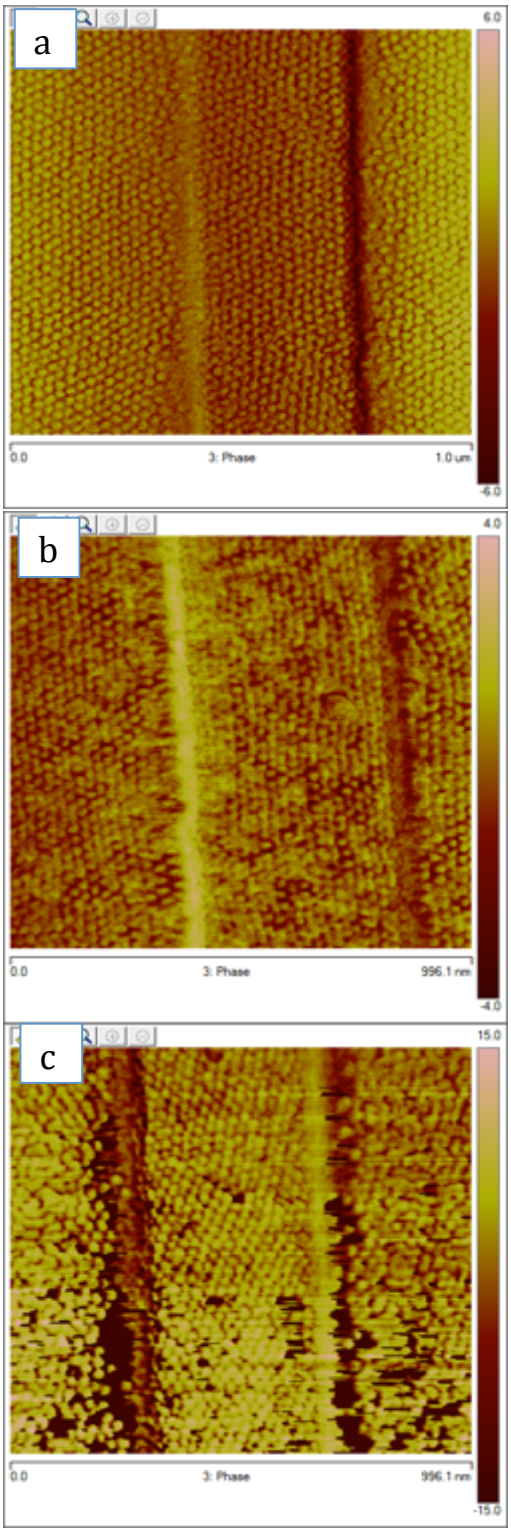

Figure 3.4 a) Block copolymer annealed in acetone vapor forms sphere morphology. b) Sphere morphology remains after lift-off photoresist in HFE solvent. c) Re-anneal in THF doesn't change the spherical morphology.

To make sure the fluorinated photoresist and solvent do not dissolve or damage the delicate morphology of the self-assembled block copolymer film, a sample was annealed in acetone vapor and cross-linked via UV radiation spin-coated fluorinated photoresist and then put into one of the stronger hydrofluoroether solvents, HFE 7600, for two minutes to lift-off the resist. As we can see from Figure 3.4 b, the spherical morphology has been retained and looks just like the original structure (Figure 3.4 a).

The patterning of the OSCoR 2312 fluorinated photoresist was performed on an ABM Contact Aligner using 365 nm UV radiation. The acid generated from the photoacid generating molecule mixed with the resist deprotects upon UV radiation the *tert*-butyl groups on the photoresist and transforms the polymer into an HFE-phobic material. The unexposed photoresist is then washed away in Orthogonal 700 developer to open windows for the subsequent oxygen plasma etching step. In this experiment, a mask containing squares and rectangules of different sizes was used. Optical microscopy images of the wafers after developing are shown in Figure 3.5. As we can see from the figure, the squares are much larger than the previous trenches and cover some parts of the trenches. Since it is difficult to do alignment patterning using the ABM, the edges of the squares are not perfectly orthogonal to the trenches.

The etching step was performed on the Oxford 81 etcher for 30 s to make sure that no block copolymer was left in the unexposed region and a sufficient amount of OSCoR 2312 remained to protect the first block copolymer layer when

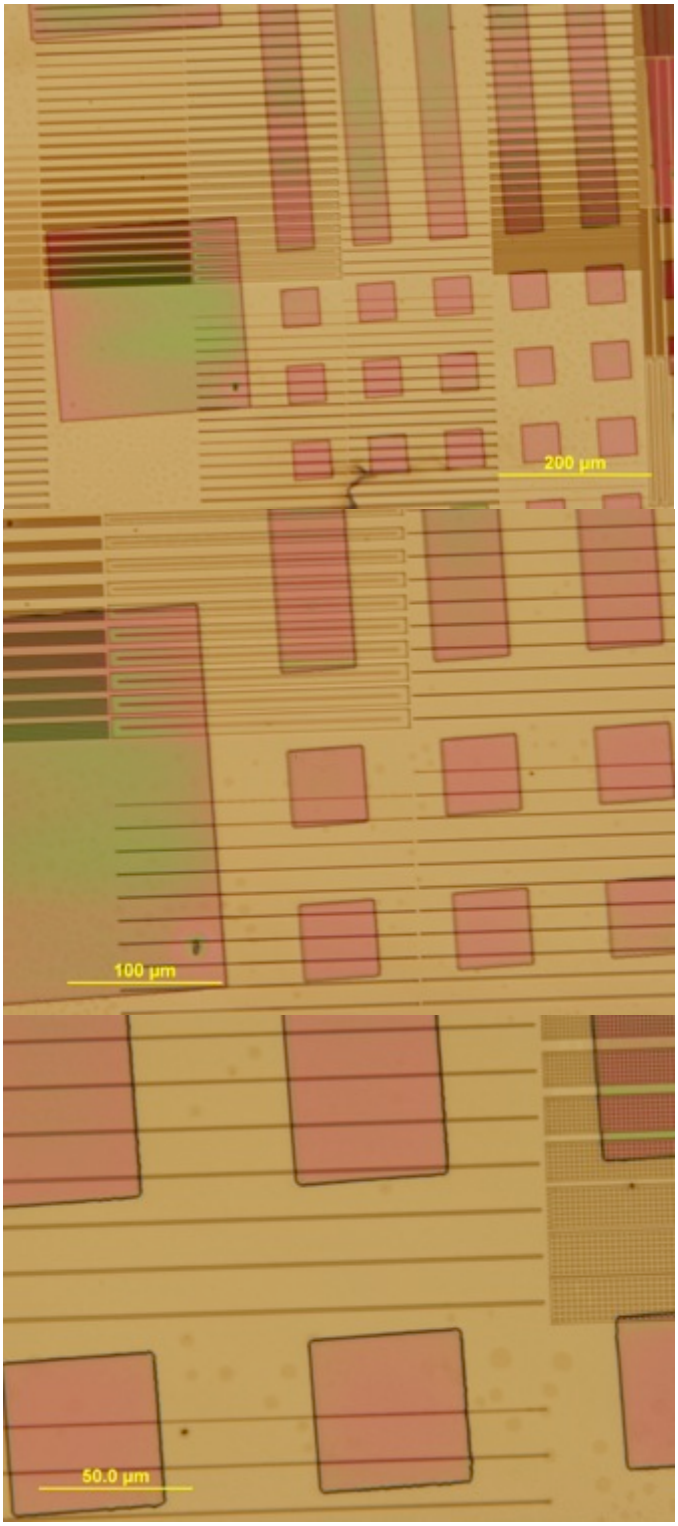

Figure 3.5 Optical microscopy images of the fluorinated resist features on top of the trenches in silicon after developing in HFE solution to wash away the unexposed regions (lighter parts).

spin-coating the second block copolymer. An approximately 850 nm thick photoresist layer is left after etching as measured by AFM.

3.3.3 HMDS treatment of the photoresist

We found that a hexamethyldisilazane (HMDS) vapor priming treatment is required of the exposed photoresist prior to the deposition of the second block copolymer for two reasons. First, the UV triggered chemistry reaction has changed the photoresist into HFE-phobic, so it is important to restore HFE solubility in order for the OSCoR 2312 to be lifted-off in HFE solutions[10]. Second, the reaction of photoresist with HMDS vapor creates a more hydrophobic surface that will prevent the adhesion of the second block copolymer during the spin coating in order for a complete removal of the photoresist.

3.3.4 Additive Patterning of the second block copolymer

Before deposition of the second block copolymer, a similar polystyrene brush treatment of the surface is performed by spin coating PS-OH from cyclohexane[20]. An overnight bake is no longer applicable since 140 °C is high enough to degrade the first block copolymer. So a short bake at 90 °C for 60 s was instead used to bond as much polystyrene brush to the wafer surface as possible. Here a poor wetting behavior of the polystyrene solution on the HMDS primed silica surface was observed since the HMDS vapor also reacts with the wafer surface and makes it more hydrophobic. However this is not a serious problem since most areas of the

film are good and were able to be used to preferentially wet the PαMS blocks of the second block copolymer.

After washing the excess polystyrene in cyclohexane, the second block copolymer (M_n=50 kg/mol) was spin-coated on top of the polystyrene brush layer. The only interaction of the PGMEA and the cross-linked first block copolymer occurs at the sidewalls of the first block copolymer film, which should not cause any significant swelling of the microdomains.

Lift-off of the photoresist must be done prior to the solvent annealing step because the solvent vapor will react with the fluorinated photoresist and make it hard to strip later. However, we still observed a longer stripping time (up to 10 min) of the fluorinated photoresist after deposition of the second block copolymer, probably due to a small amount of block copolymer film covering the top of the photoresist layer and blocking the entry of the stripper solvent into the resist. In addition to the solvent lift-off process, flushing the wafer with stripping solvent for several minutes is needed to completely remove all the photoresist, leaving the first and second block copolymer regions adjacent to each other within a single layer.

The second solvent annealing step is performed in acetone vapor using the flow chamber described in the previous chapter. The initial thickness measured by the Filmetrics device is 66.9 nm and the film is swelled to a thickness of 137.5 nm (205 %) to gain the desired morphology in the uncross-linked region of the second block copolymer. After solvent annealing, the film was exposed to 254 nm UV radiation for 10 min and baked at 115 °C for 60 s to cross-link and lock the morphology.

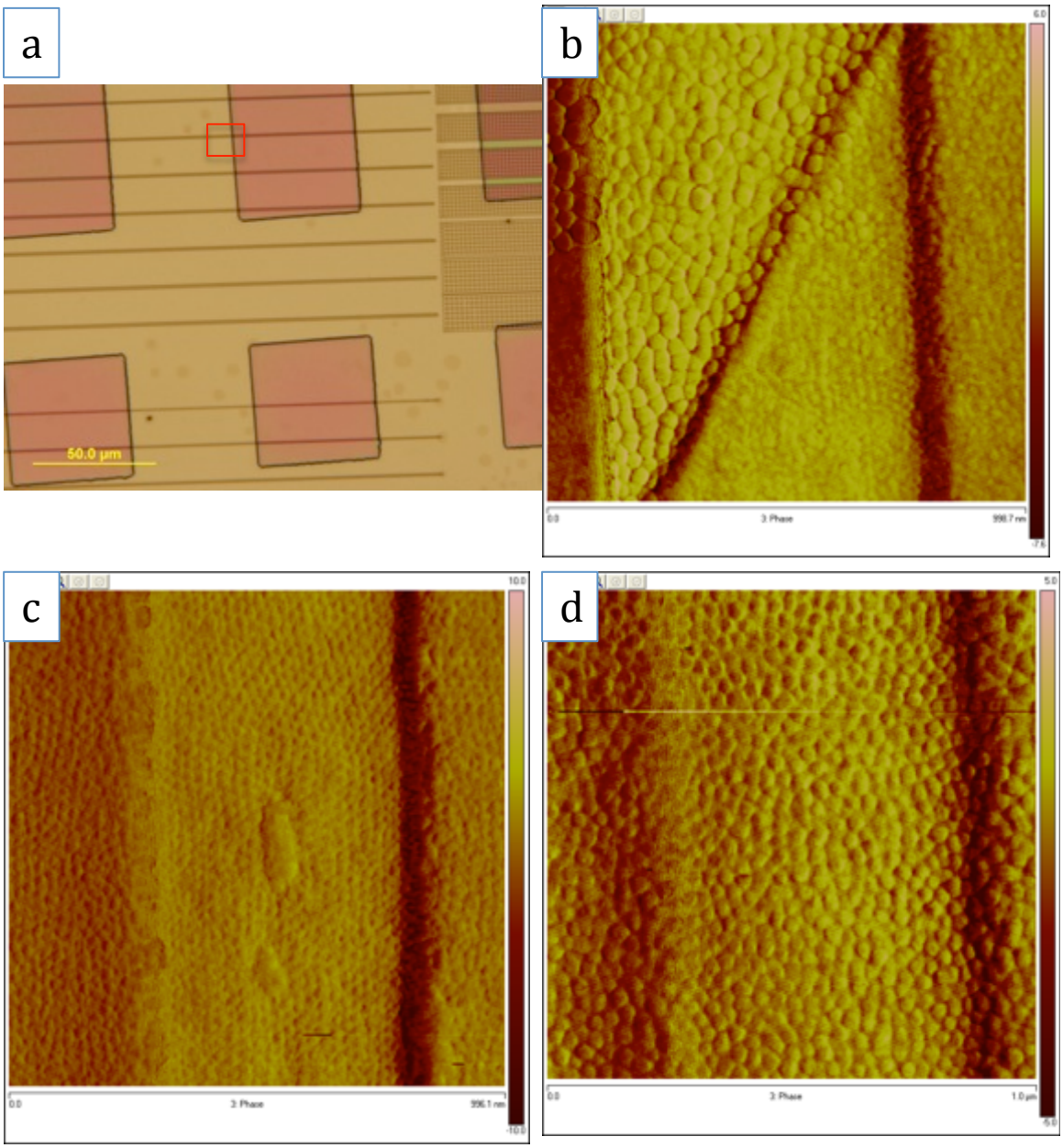

Figure 3.6 a) Optical microscopy of the patterns. b) AFM phase taken at the edge of the two block copolymer regions. c) AFM phase image shows the morphology in the first block copolymer region (pink squares). d) AFM phase image shows the morphology in the second block copolymer region (lighter parts).

AFM images of the respective block copolymer morphologies located in each region of the wafer are shown in Figure 3.6. Here we used two block copolymers with different molecular weights, but that yield the same spherical morphology to demonstrate the ability to pattern multiple block copolymers within one layer. The size of the self-assembled patterns are determined by the molecular weight, and thus in the first block copolymer region (Figure 3.6 c), the diameter of the spheres is ~18 nm compared to the much larger spheres (~30 nm) in the second block copolymer region (Figure 3.6 d). Figure 3.6 b shows an AFM image taken on the edge between the two block copolymer regions and clearly demonstrates two different sizes of microdomains that are adjacent to each other on the same layer without significant intermixing.

The morphology of the first block copolymer region is not as clear since the film had been soaked and flushed in HFE solution for a long time. This could potentially be solved by finding another patterning step on tools other than ABM to lower the dose used and make the photoresist easier to lift-off after patterning. Future work can be done by creating two different morphologies (cylinder and sphere) within one layer, and transferring the patterns to the substrate after removing of the PαMS blocks.

3.4 Conclusion

Here we demonstrate a novel patterning process, which allows for patterning multiple block copolymers with different sizes and pitches adjacent to each other within a single layer without damaging or intermixing. The morphology is first

cross-linked and locked by a UV triggered crosslinking reaction by adding a small amount of PAG and cross-linker. And then a fluorinated photoresist and solvent, which neatly bypass the intermixing problem between different layers, are used to create windows in the first block copolymer layer. The second block copolymer is spin-coated to cover those areas and solvent annealed to gain the desired morphology. This orthogonal patterning method could be applied to other block copolymer systems and expands the potential of the block copolymer self-assembly application in device fabrication.

3.5 Acknowledgement

This work is supported by the National Science Foundation. The author would like to thank Carol Newby for the help with the lithography patterning steps, Hee-Soo Yoo for synthesis of the block copolymer and Michelle Chavis for the help with the flow chamber. This work was performed using facilities at the Cornell NanoScale Facility (CNF), a member of the National Nanotechnology Infrastructure Network, which is supported by the National Science Foundation (Grant ECS-03335765).

REFERENCES

1. Black, C.T., Polymer self-assembly as a novel extension to optical lithography. *Acs Nano* **2007**, 1, 147-150.
2. Mansky, P., et al., Controlling polymer-surface interactions with random copolymer brushes. *Science* **1997**, 275, 1458-1460.
3. Mansky, P., et al., Ordered diblock copolymer films on random copolymer brushes. *Macromolecules* **1997**, 30, 6810-6813.
4. Huang, E., et al., Neutrality conditions for block copolymer systems on random copolymer brush surfaces. *Macromolecules* **1999**, 32, 5299-5303.
5. Ryu, D.Y., et al., A generalized approach to the modification of solid surfaces. *Science* **2005**, 308, 236-239.
6. Bang, J., et al., Facile routes to patterned surface neutralization layers for block copolymer lithography. *Advanced Materials* **2007**, 19, 4552-+.
7. Han, E., et al., Photopatternable imaging layers for controlling block copolymer microdomain orientation. *Advanced Materials* **2007**, 19, 4448-+.
8. Han, E., et al., Effect of Composition of Substrate-Modifying Random Copolymers on the Orientation of Symmetric and Asymmetric Diblock Copolymer Domains. *Macromolecules* **2008**, 41, 9090-9097.
9. Bosworth, J.K., C.T. Black, and C.K. Obert, Selective Area Control of Self-Assembled Pattern Architecture Using a Lithographically Patternable Block Copolymer. *Acs Nano* **2009**, 3, 1761-1766.
10. Hwang, H.S., et al., Dry photolithographic patterning process for organic electronic devices using supercritical carbon dioxide as a solvent. *Journal of Materials Chemistry* **2008**, 18, 3087-3090.
11. Lee, J.K., et al., Acid-sensitive semiperfluoroalkyl resorcinarene: An imaging material for organic electronics. *Journal of the American Chemical Society* **2008**, 130, 11564-+.
12. Lee, J.K., et al., Semiperfluoroalkyl Polyfluorenes for Orthogonal Processing in Fluorous Solvents. *Macromolecules* **2010**, 43, 1195-1198.

13. Taylor, P.C., et al., Orthogonal Patterning of PEDOT:PSS for Organic Electronics using Hydrofluoroether Solvents. *Advanced Materials* **2009**, 21, 2314-+.
14. Zakhidov, A.A., et al., Hydrofluoroethers as orthogonal solvents for the chemical processing of organic electronic materials. *Advanced Materials* **2008**, 20, 3481-+.
15. Li, M.Q., et al., Spatially controlled fabrication of nanoporous block copolymers. *Chemistry of Materials* **2004**, 16, 3800-3808.
16. Paik, M.Y., et al., Reversible Morphology Control in Block Copolymer Films via Solvent Vapor Processing: An in Situ GISAXS Study. *Macromolecules* **2010**, 43, 4253-4260.
17. Ito, H., Chemical amplification resists: Inception, implementation in device manufacture, and new developments. *Journal of Polymer Science Part a-Polymer Chemistry* **2003**, 41, 3863-3870.
18. Qinghuang Lin, A.D.K.a.C.G.W., Effects of crosslinking agent on lithographic performance of negative-tone resists based on poly(p-hydroxystyrene). *Proc. SPIE* **1997**, 3049, 974.
19. Horst Roeschert, R.R.D., Charlotte Eckes, K. Kamiya, Winfried Meier, Klaus J. Przybilla, Walter Spiess and Georg Pawlowski, DN 21, DN 41: negative-tone photoresists for deep-UV lithography. *Proc. SPIE* **1992**, 1672, 157.
20. Harrison, C., et al., Reducing substrate pinning of block copolymer microdomains with a buffer layer of polymer brushes. *Macromolecules* **2000**, 33, 857-865.